Inorganic Chemistry

Article

Effective Control of Ligation and Geometric Isomerism: Direct Comparison of Steric Properties Associated with Bis-mesityl and Bis-diisopropylphenyl *m*-Terphenyl Isocyanides

Treffly B. Ditri, Brian J. Fox, Curtis E. Moore, Arnold L. Rheingold, and Joshua S. Figueroa*

Department of Chemistry and Biochemistry, University of California, San Diego, 9500 Gilman Drive, Mail Code 0358, La Jolla, California 92093-0358

A synthetic procedure for the sterically encumbered *m*-terphenyl isocyanide CNAr^{Dipp2} (Dipp = 2,6-diisopropylphenyl) is presented. In comparison to the less encumbering *m*-terphenyl isocyanide ligand CNAr^{Mes2}, the steric attributes of the flanking Dipp groups effectively control the extent of CNAr^{Dipp2} ligation to monovalent Cu and Ag centers and zero-valent Mo centers. Direct structural comparisons of Cu(I) and Ag(I) complexes of both CNAr^{Dipp2} and CNAr^{Mes2} are made. It was found that only two CNAr^{Dipp2} ligands are accommodated by monovalent Cu and Ag centers, whereas three CNAr^{Mes2} units can readily bind. As demonstrated by both ^{1}H NMR and FTIR spectroscopic studies, addition of a third equivalent of CNAr^{Dipp2} to [(THF)$_2$Cu(CNAr^{Dipp2})$_2$]OTf in C$_6$D$_6$ solution results in slow isocyanide exchange. However, rapid isocyanide exchange is observed when an additional equivalent of CNAr^{Dipp2} is added to (TfO)Ag(CNAr^{Dipp2})$_2$. Three CNAr^{Mes2} ligands react smoothly with *fac*-Mo(CO)$_3$(NCMe)$_3$ to afford the octahedral complex *fac*-Mo(CO)$_3$(CNAr^{Mes2})$_3$, which can be converted irreversibly to the *mer* isomer upon heating in solution. Contrastingly, addition of CNAr^{Dipp2} to *fac*-Mo(CO)$_3$(NCMe)$_3$ results in a mixture of both the tetracarbonyl and the tricarbonyl complexes *trans*-Mo(CO)$_4$(CNAr^{Dipp2})$_2$ and *trans*-Mo(NCMe)(CO)$_3$(CNAr^{Dipp2})$_2$, respectively, in which the encumbering CNAr^{Dipp2} ligands are in a *trans*-disposition. Ultraviolet irradiation of the preceding mixture in NCMe/Et$_2$O under an argon flow provides exclusively the tricarbonyl complex *trans*-Mo(NCMe)(CO)$_3$(CNAr^{Dipp2})$_2$. Addition of free CNAr^{Dipp2} to *trans*-Mo(NCMe)(CO)$_3$(CNAr^{Dipp2})$_2$ does not result in the binding of a third isocyanide unit by the Mo center as determined by ^{1}H NMR spectroscopy. Treatment of *trans*-Mo(NCMe)(CO)$_3$(CNAr^{Dipp2})$_2$ with the Lewis base pyridine (py) affords the complex *fac,cis*-Mo(py)(CO)$_3$(CNAr^{Dipp2})$_2$ as determined by X-ray diffraction. Notably, the encumbering nature of the CNAr^{Dipp2} units forces a *cis* C$_{iso}$—Mo—C$_{iso}$ angle of about 100°.

Introduction

Isocyanides (C≡NR) have long been recognized as effective ligands for transition metals because of their standing as isolobal fragments to carbon monoxide (CO).[1] Accordingly, this electronic structure attribute has enabled the use of isocyanides as tunable organic surrogates to CO within a host of low-valent metal complexes. For example, 18-electron homoleptic isocyanometallates[2,3] of Fe and Co have been prepared (e.g., [Fe(CNXyl)$_4$]$^{2-}$ and [Co(CNXyl)$_4$]$^-$, Xyl = 2,6-Me$_2$C$_6$H$_3$), which are clear analogues of the well-known carbonylmetallates [Fe(CO)$_4$]$^{2-}$ and [Co(CO)$_4$]$^-$. In addition, homoleptic isocyanide complexes of the Group 6 metals, akin to the classic M(CO)$_6$ series of compounds, have been reported.[4] Most interestingly however, metal isocyanides and isocyanometallates often display reactivity patterns distinct from their carbonyl congeners owing to the attenuated π-acidity and increased σ-basicity of the C≡NR function relative to CO.[1,5]

*To whom correspondence should be addressed. E-mail: jsfig@ucsd.edu.

(1) (a) Malatesta, L.; Bonati, F. *Isocyanide Complexes of Transition Metals*; Wiley: New York, 1969. (b) Bonati, F.; Minghetti, G. *Inorg. Chim. Acta* **1974**, *9*, 95–112. (c) Sarapu, A. C.; Fenske, R. F. *Inorg. Chem.* **1974**, *14*, 247–253. (d) Yamamoto, Y. *Coord. Chem. Rev.* **1980**, *32*, 193–233.

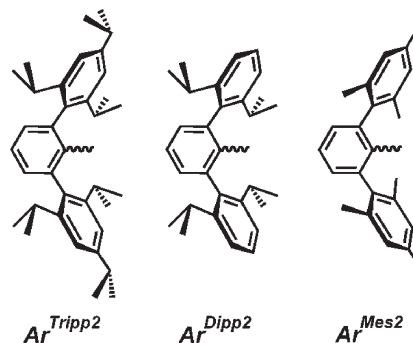(2) Brennessel, W. W.; Ellis, J. E. *Angew. Chem., Int. Ed.* **2007**, *46*, 598–600.

(3) (a) Warnock, G. F.; Cooper, N. J. *Organometallics* **1989**, *8*, 1826–1827. (b) Leach, P. A.; Geib, S. J.; Corella, J. A.; Warnock, G. F.; Cooper, N. J. *J. Am. Chem. Soc.* **1994**, *116*, 8566–8574.

(4) (a) Mann, K .R.; Cimolino, M.; Geoffroy, G. L.; Hammond, G. S.; Orio, A. A.; Albertin, G.; Gray, H. B. *Inorg. Chim. Acta* **1976**, *16*, 97–101. (b) Treichel, P. M.; Essenmacher, G. J. *Inorg. Chem.* **1976**, *15*, 146–150. (c) Chiu, K. W.; Jones, R. A.; Wilkinson, G.; Galas, A. M. R.; Hursthouse, M. B. *J. Chem. Soc., Dalton Trans.* **1981**, 2088–2097. (d) Yamamoto, Y.; Yamazaki, H. *J. Organomet. Chem.* **1985**, *282*, 191–200. (e) Carnahan, E. M.; Lippard, S. J. *J. Chem. Soc., Dalton Trans.* **1991**, 699–706. (f) Acho, J. A.; Lippard, S. J. *Organometallics* **1994**, *13*, 1294–1299. (g) Barybin, M. V.; Holovics, T. C.; Deplazes, S. F.; Lushington, G. H.; Powell, D. R.; Toriyama, M. *J. Am. Chem. Soc.* **2002**, *124*, 13668–13669. (h) Robinson, R. E.; Holovics, T. C.; Deplazes, S. F.; Lushington, G. H.; Powell, Barybin, M. V *J. Am. Chem. Soc.* **2003**, *125*, 4432–4433.

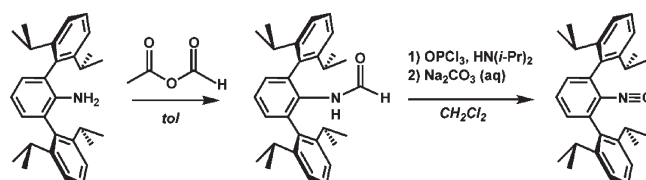(5) Weber, L. *Angew. Chem., Int. Ed.* **1998**, *37*, 1515–1517.

Seeking to further enhance the reactivity of isocyanide complexes by enforcing low metal coordination numbers, we have recently introduced the sterically encumbering bis-mesityl substituted *m*-terphenyl isocyanide ligand CNAr^{Mes2} (Mes = 2,4,6-Me$_3$C$_6$H$_2$).[6] It was demonstrated that the CNAr^{Mes2} ligand affords tris-isocyanide Cu(I) species under conditions where *tetrakis*-isocyanide Cu(I) complexes are normally obtained. Thus, in comparison to less sterically protective C≡NR ligands, the spatial properties of CNAr^{Mes2} can effectively prevent maximal isocyanide ligation with respect to a given metal center. The ability of the *m*-terphenyl framework[7] to significantly affect the structure and reactivity of transition-metal and main-group atoms is well established.[7−10] For example, Power has recently demonstrated that certain hindered *m*-terphenyl ligands can kinetically stabilize remarkably low-coordinate Cr monomers,[11] whereas less encumbering *m*-terphenyls give rise to Cr−Cr dimers with 5-fold bonding interactions.[11b,12] Furthermore, Protasiewicz has reported an elegant intermolecular chlorine-atom transfer reaction, which is thermodynamically controlled by the steric properties of the *m*-terphenyl group.[13] In this latter work, it was shown that phosphorus atoms bearing the Ar^{Mes2} *m*-terphenyl group more readily accommodate a higher coordination number than those featuring the larger bis-triisopropylphenyl derivative Ar^{Tripp2} (Tripp = 2,4,6-(*i*-Pr)$_3$C$_6$H$_2$, see Chart 1).

Inspired by these studies, we sought to generate additional encumbering *m*-terphenyl isocyanides to compare the effect of the Ar^{R2} group on the relative coordination behavior of the isocyanide functionality and structural properties of ensuing complexes. We hoped that by increasing the steric demand of the *m*-terphenyl framework, lower-coordinate metal complexes may be prepared which are otherwise inaccessible with our prototype CNAr^{Mes2} system. Furthermore, we were particularly curious if the spacing provided by

(6) Fox, B. J.; Sun, Q. Y.; DiPasquale, A. G.; Fox, A. R.; Rheingold, A. L.; Figueroa, J. S. *Inorg. Chem.* **2008**, *47*, 9010–9020.

(7) (a) Twamley, B.; Haubrich, S. T.; Power, P. P. *Adv. Organomet. Chem.* **1999**, *44*, 1–65. (b) Clyburne, J. A. C.; McMullen, N. *Coord. Chem. Rev.* **2000**, *210*, 73–99.

(8) For representative papers detailing the effect of differently substituted *m*-terphenyl ligands on structure, see: (a) Li, X.-W.; Pennington, W. T.; Robinson, G. H. *J. Am. Chem. Soc.* **1995**, *117*, 7578–7579. (b) Wehmschulte, R. J.; Grigsby, W. J.; Schiemenz, B.; Bartlett, R. A.; Power, P. P. *Inorg. Chem.* **1996**, *35*, 6694–6702. (c) Su, J.; Li, X.-W.; Crittendon, C.; Robinson, G. H. *J. Am. Chem. Soc.* **1997**, *119*, 5471–5472. (d) Phillips, A. D.; Wright, R. J.; Olmstead, M. M.; Power, P. P. *J. Am. Chem. Soc.* **2002**, *124*, 5930–5931.

(9) For additional reviews and perspectives, see: (a) Power, P. P. *Chem. Rev.* **1999**, *99*, 3463–3504. (b) Robinson, G. H. *Acc. Chem. Res.* **1999**, *32*, 773–782. (b) Robinson, G. H. *Chem. Commun.* **2000**, 2175–2181. (c) Power, P. P. *Chem. Commun.* **2003**, 2091–2101. (d) Power, P. P. *Organometallics* **2007**, *26*, 4362–4372. (e) Rivard, E.; Power, P. P. *Inorg. Chem.* **2007**, *46*, 10047–10064.

(10) For representative applications to transition and main group elements, see: (a) Shah, S.; Simpson, M. C.; Smith, R. C.; Protasiewicz, J. D. *J. Am. Chem. Soc.* **2001**, *123*, 6925–6926. (b) Gavenonis, J.; Tilley, T. D. *Organometallics* **2002**, *21*, 5549–5563. (c) Waterman, R.; Hillhouse, G. L. *Organometallics* **2003**, *22*, 5182–5184. (d) Gavenonis, J.; Tilley, T. D. *Organometallics* **2004**, *23*, 31–43. (e) Filippou, A. C.; Weidemann, N.; Philippopoulos, A. I.; Schnakenburg, G. *Angew. Chem., Int. Ed. Engl.* **2006**, *45*, 5987–5991. (f) Carson, E. C.; Lippard, S. J. *Inorg. Chem.* **2006**, *45*, 828–836. (g) Klein, D. P.; Young, V. G.; Tolman, W. B.; Que, L. *Inorg. Chem.* **2006**, *45*, 8006–8008.

(11) (a) Wolf, R.; Brynda, M.; Ni, C.; Long, G. J.; Power, P. P. *J. Am. Chem. Soc.* **2007**, *129*, 6076–6077. (b) Wolf, R.; Ni, C.; Nguyen, T.; Brynda, M.; Long, G. J.; Sutton, A. D.; Fischer, R. C.; Fettinger, J. C.; Hellman, M.; Pu, L.; Power, P. P. *Inorg. Chem.* **2007**, *46*, 11277–11290.

(12) Nguyen, T.; Sutton, A. D.; Brynda, M.; Fettinger, J. C.; Long, G. J.; Power, P. P. *Science* **2005**, *310*, 844–847.

(13) Smith, R. C.; Shah, S.; Urnezius, E.; Protasiewicz, J. D. *J. Am. Chem. Soc.* **2003**, *125*, 40–41.

Chart 1. Common Substituted *m*-Terphenyl Frameworks

Ar^{Tripp2}　　　　Ar^{Dipp2}　　　　Ar^{Mes2}

Scheme 1

the two-atom, isocyanide linkage would serve to negate any added steric influence of the *m*-terphenyl group. Such long metal-to-bulk distances could potentially render the steric properties of various flanking substituents of an *m*-terphenyl unit identical. Accordingly, herein we present a new *m*-terphenyl isocyanide variant, namely, the bis-diisopropyl-phenyl derivative[7,14] CNAr^{Dipp2} (Dipp = 2,6-(*i*-Pr)$_2$C$_6$H$_3$), and show that relative to CNAr^{Mes2}, its increased steric demand is indeed significant, and further controls the extent of isocyanide ligation for Group 11 metal centers. In addition, we have investigated the relative coordination behavior of both CNAr^{Mes2} and CNAr^{Dipp2} toward zero-valent molybdenum−carbonyl fragments ([Mo(CO)$_n$], n = 3,4). As with the Group 11 metals surveyed, CNAr^{Mes2} and CNAr^{Dipp2} differ in the extent of their ligation to these reduced molybdenum centers. However, both *m*-terphenyl isocyanides dramatically affect the coordination geometry of the resulting molybdenum complexes and are shown to provide geometric isomers that are exceptionally rare in the context of mixed isocyanide/carbonyl Group 6 species.

Results and Discussion

Preparation of the *m*-Terphenyl Isocyanide CNAr^{Dipp2}. A synthetic route to CNAr^{Dipp2} is outlined in Scheme 1. Unlike the synthesis of CNAr^{Mes2},[6] the steric properties of the Ar^{Dipp2} framework prevent a smooth condensation reaction between the aniline[15] H$_2$NAr^{Dipp2} and formic acid (HC(O)OH). We thus turned to the potent electrophile acetic formic anhydride (H$_3$CC(O)OC(O)H),[16] which successfully effected the formylation of H$_2$N-Ar^{Dipp2} in high yield over the course of 36 h. Dehydration of the corresponding formaniline HC(O)HNAr^{Dipp2} with

(14) Schiemenz, B.; Power, P. P. *Angew. Chem., Int. Ed.* **1996**, *35*, 2150–2152.

(15) The aniline H$_2$NAr^{Dipp2} has been reported previously, but a detailed synthesis was not disclosed. We therefore present full details of its preparation and characterization in the Experimental Section. See: Li, J.; Song, H.; Cui, C.; Cheng, J.-P *Inorg. Chem.* **2008**, *47*, 3468–3470.

(16) (a) Huffman, C. W. *J. Org. Chem.* **1958**, *23*, 727–729. (b) Krimen, L. I. *Org. Synth.* **1970**, *50*, 1–3.
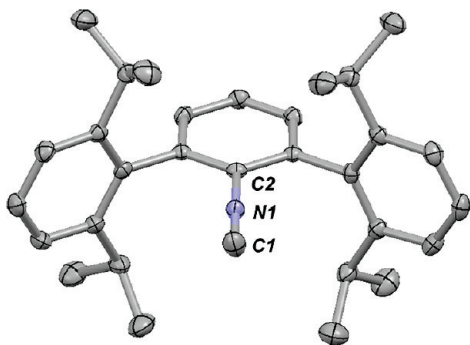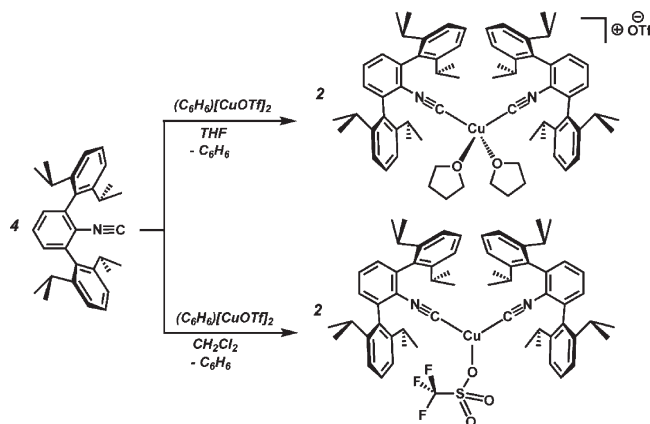
Figure 1. Molecular structure of CNAr^{Dipp2}. Selected bond distances (Å) and angles (deg): C1−N1 = 1.1577(18); N1−C2 = 1.4009(16); C1−N1−C2 = 176.72(13).

Scheme 2

OPCl$_3$ in the presence of HN(i-Pr)$_2$ proceeded readily to afford isocyanide CNAr^{Dipp2} in 90% yield. Crystallographic characterization of CNAr^{Dipp2} confirmed the presence of the isocyano group (d(C1−N1) = 1.1577(18) Å, Figure 1), as did FTIR spectroscopy, which revealed solid-state (KBr) and solution (C$_6$D$_6$) $\nu_{(CN)}$ stretches of 2124 cm^{-1} and 2118 cm^{-1}, respectively.

Coordination Platforms Lacking Significant π-Basicity: Monovalent Cu and Ag Centers. The steric differences between CNAr^{Dipp2} and CNAr^{Mes2} are immediately evidenced by their coordination behavior toward the Cu(I) triflate fragment. In the case of CNAr^{Mes2}, the tris-isocyanide salt [(THF)Cu(CNAr^{Mes2})$_3$]OTf (OTf = [OSO$_2$CF$_3$]$^-$) was readily obtained upon its combination with (C$_6$H$_6$)[Cu(OTf)]$_2$ in tetrahydrofuran (THF) solution.[6] Contrastingly, the sterically expanded CNAr^{Dipp2} ligand permits only the isolation of bis-isocyanide Cu(I) monomers. As depicted in Scheme 2, addition of 4.0 equiv of CNAr^{Dipp2} to (C$_6$H$_6$)[Cu(OTf)]$_2$ in THF results in the formation of the salt, [(THF)$_2$Cu(CNAr^{Dipp2})$_2$]OTf, as a colorless crystalline solid in 62% isolated yield. Structural characterization of [(THF)$_2$Cu(CNAr^{Dipp2})$_2$]OTf by X-ray diffraction (Figure 2) confirmed the non-coordinating nature of OTf$^-$ counterion when two THF ligands are present in the Cu primary coordination sphere. Most importantly, however, treatment of pure [(THF)$_2$Cu(CNAr^{Dipp2})$_2$]OTf with an additional equivalent of CNAr^{Dipp2} does not lead to a tris-isocyanide complex. Instead, analysis of 1:1 [(THF)$_2$-Cu(CNAr^{Dipp2})$_2$]OTf/CNAr^{Dipp2} mixtures by ^{1}H NMR spectroscopy (C$_6$D$_6$) revealed slightly broadened reso-
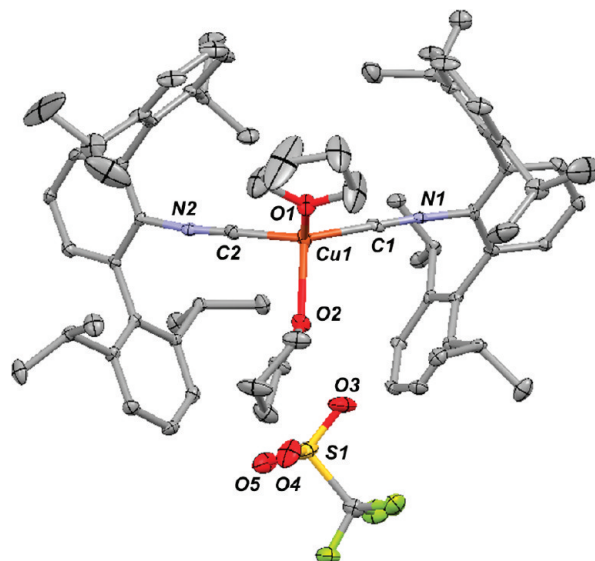
Figure 2. Molecular structure of [(THF)$_2$Cu(CNAr^{Dipp2})$_2$]OTf. Selected bond distances (Å) and angles (deg): Cu3−C1 = 1.902(5); Cu1−C2 = 1.903(5); Cu1−O1 = 2.125(3); Cu1−O2 = 2.187(3); C1−Cu1−C2 = 135.16(19); C1−Cu1−O1 = 103.57(16); C2−Cu1−O1 = 109.62(16); C1−Cu1−O2 = 107.95(16); C2−Cu1−O2 = 99.69(16); O1−Cu1−O2 = 92.92(12). C1−N2−C11(ipso) = 175.9(4); C2−N1−C42(ipso) = 171.2(4).

nances for the two reactants indicative of a slow isocyanide exchange process on the ^{1}H NMR time scale. Solution FTIR spectroscopic studies (C$_6$D$_6$) on these mixtures revealed $\nu_{(CN)}$ stretches corresponding only to [(THF)$_2$Cu(CNAr^{Dipp2})$_2$]OTf and free CNAr^{Dipp2}, thereby corroborating the notion that a tris-CNAr^{Dipp2} species is not formed to an appreciable extent.

The resistance of [(THF)$_2$Cu(CNAr^{Dipp2})$_2$]OTf toward binding a third CNAr^{Dipp2} ligand can be readily traced to the encumbering nature of the flanking Dipp units.[8b] As revealed by the molecular structure of [(THF)$_2$Cu-(CNAr^{Dipp2})$_2$]OTf (Figure 2), the steric congestion posed by these fragments forces a markedly expanded C(1)−Cu−C(2) angle of 135.16(19)° in the nominally four-coordinate d^{10} Cu(I) center. In comparison, the largest angle found for [(THF)Cu(CNAr^{Mes2})$_3$]OTf, which possesses three less encumbering CNAr^{Mes2} ligands, is 119.14(13)°. Notably for [(THF)$_2$Cu(CNAr^{Dipp2})$_2$]OTf, the C$_{iso}$−N−C$_{aryl}$ angles in each CNAr^{Dipp2} ligand retain a near linear disposition. This observation is consistent with the absence of significant π-back bonding from the Cu(I) center,[17] and thus reflects the fact that electronic factors (i.e., isocyanide bending as induced by π back-bonding) do not aid in maximizing the distance between the two Ar^{Dipp2} substituents. Thus we contend that the C$_{iso}$−Cu−C$_{iso}$ angle simply expands to minimize steric interferences between the large CNAr^{Dipp2} units. Accordingly, the inability of [(THF)$_2$Cu(CNAr^{Dipp2})$_2$]OTf to bind a third CNAr^{Dipp2} unit can be rationalized by the impossibility

(17) This notion is also supported by solid state (KBr) and solution (C$_6$D$_6$) FTIR spectra of [(THF)$_2$Cu(CNAr^{Dipp2})$_2$]OTf, which reveal $\nu_{(CN)}$ stretches of 2167 cm^{-1} and 2165 cm^{-1}, respectively. Such shifts to higher energy from that of free CNAr^{Dipp2} (2124 cm^{-1} (KBr) and 2118 cm^{-1} (C$_6$D$_6$)) are consistent with predominate isocyanide σ-donation concomitant with a minimal back bonding interaction. See: (a) Robertson, M. J.; Angelici, R. J. *Langmuir* **1994**, *10*, 1488−1492. (b) Shih, K.; Angelici, R. J. *Langmuir* **1995**, *11*, 2539−2546. (c) Henderson, J. I.; Feng, S.; Bein, T.; Kubiak, C. P. *Langmuir* **2000**, *16*, 6183−6187.
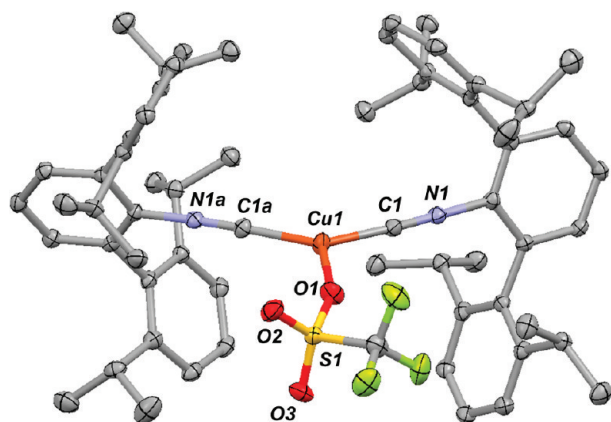
Figure 3. Molecular structure of (TfO)Cu(CNAr^{Dipp2})$_2$. Selected bond distances (Å) and angles (deg): C1−Cu1 = 1.884(4); Cu1−O1 = 2.082(4); C1−Cu1−C1a = 138.5(2); C1−Cu1−O1 = 110.77(12); S1−O1−Cu1 = 152.91(11); C1−N1−C2(ipso) = 177.1(4).

of accommodating three 120° or greater C$_{iso}$−M−C$_{iso}$ bond angles within a trigonal or pseudotetrahedral coordination geometry. Contrastingly, three C$_{iso}$−M−C$_{iso}$ bond angles of 120° or less are readily accommodated within the CNAr^{Mes2} system, resulting in stable tris-isocyanide complexes. In addition, the steric influences attendant within the [Cu(CNAr^{Dipp2})$_2$] fragment are consistent irrespective of the coordination number at Cu or the nature of the other ligands present. This fact is demonstrated by the structural characterization of the solvent-free triflate complex, (κ^1-TfO)Cu(CNAr^{Dipp2})$_2$, which possesses a significantly expanded C(1)−Cu−C(2) angle of 138.5(2)° for a nominally three-coordinate, Cu(I) complex featuring only monodentate ligands (Figure 3, Scheme 2).[18]

The steric interference posed by the CNAr^{Dipp2} framework is also not overcome by moderate changes in M−C$_{iso}$ bond lengths. Accordingly, in an attempt to increase the likelihood of obtaining a tris-CNAr^{Dipp2} Group 11 complex, we postulated that a Ag(I) center, with its larger covalent radius relative to that of Cu(I),[19] may possibly allow the ligation of three encumbering isocyanide units. As with the [CuOTf] fragment, three of the relatively smaller CNAr^{Mes2} ligands are easily accommodated within the primary coordination sphere of Ag(I). Thus, treatment of AgOTf with 3 equiv of CNAr^{Mes2} in THF solution affords the tris-isocyanide salt [(THF)Ag(CNAr^{Mes2})$_3$]OTf as assayed by ^{1}H NMR spectroscopy (C$_6$D$_6$, Scheme 3).

(18) A search of the Cambridge Structural Database (CSD v. 5.30, Nov. 2008) for three-coordinate Cu complexes, and refined only to those featuring only monodentate ligands, resulted in approximately 200 hits. Of these, roughly 10 complexes contained ligand−Cu−ligand angles greater than 139°. Furthermore, the majority of the complexes displaying such large angles featured two sterically encumbering P(benzyl)$_3$ and P(Cy)$_3$ ligands (cone angle θ = 165° and 170°, respectively, see:Tolman, C. A. *Chem. Rev.* **1977**, *77*, 313–348 See the Supporting Information for additional details, and (a) Restivo, R. J.; Costin, A.; Ferguson, G.; Carty, A. J. *Can. J. Chem.* **1975**, *53*, 1949–1957. (b) Green, J.; Sinn, E.; Woodward, S.; Butcher, R. *Polyhedron* **1993**, *12*, 991–1001. (c) Darensbourg, D. J.; Holtcamp, M. W.; Longridge, E. M.; Khandelwal, B.; Klausmeyer, K. K.; Reibenspies, J. H. *J. Am. Chem. Soc.* **1995**, *117*, 318–328. (d) Ainscough, E. W.; Brodie, A. M.; Burrell, A. K.; Freeman, G. F.; Jameson, G. B.; Bowmaker, G. A.; Hanna, J. V.; Healy, P. C. *Dalton. Trans.* **2001**, 144–151. (e) Lobbia, G. G.; Pellei, M.; Pettinari, C.; Santini, C.; Somers, N.; White, A. H. *Inorg. Chim. Acta* **2002**, *333*, 100–108.

(19) As derived from metal hydrides, the covalent radii of Cu and Ag are tabulated as, 1.11 Å and 1.26 Å, respectively. See:Batsanov, S. S. *Rus. Chem. Bull.* **1995**, *45*, 2245–2250.

Scheme 3
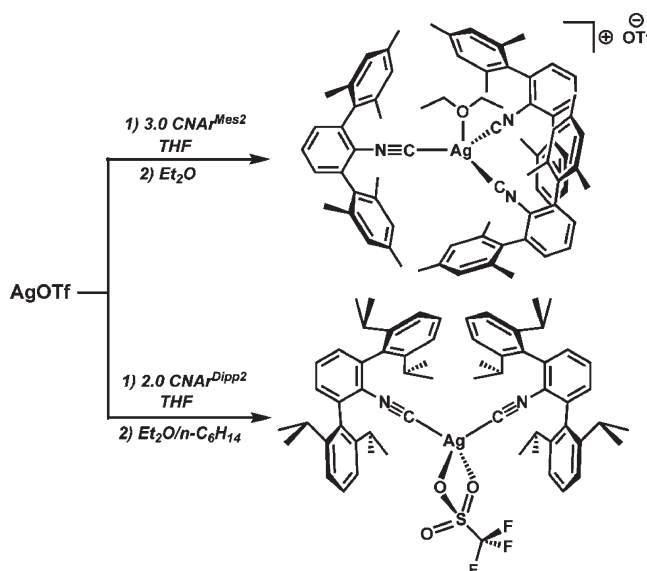
Dissolution of [(THF)Ag(CNAr^{Mes2})$_3$]OTf in Et$_2$O results in solvent exchange, affording the salt [(Et$_2$O)-Ag(CNAr^{Mes2})$_3$]OTf, which was subjected to structural characterization (Figure 4). In contrast to CNAr^{Mes2}, however, ligation of three CNAr^{Dipp2} ligands is in fact resisted by Ag(I) centers. For example, treatment of AgOTf with 2.0 equiv of CNAr^{Dipp2} in THF, followed by crystallization of the resultant solids from an Et$_2$O/*n*-hexane mixture, provides the solvent-free complex (TfO)-Ag(CNAr^{Dipp2})$_2$ (Scheme 3). The molecular structure of (OTf)Ag(CNAr^{Dipp2})$_2$ has been determined by X-ray diffraction and is shown in Figure 5. In contrast to its Cu(I) analogue, a bidentate, κ^2 binding mode is observed for the triflate unit in (OTf)Ag(CNAr^{Dipp2})$_2$, but an expanded C$_{iso}$−Ag1−C$_{iso}$ angle of 142.2(2)° is still observed. As determined by both ^{1}H NMR and FTIR spectroscopy, however, treatment of (κ^2-TfO)Ag(CNAr^{Dipp2})$_2$ with an additional equivalent of CNAr^{Dipp2} in C$_6$D$_6$ results in fast exchange between free and coordinated isocyanide but does not lead to a stable tris-isocyanide.[20]

Coordination Platforms Featuring Significant π-Basicity: Mixed Isocyanide/Carbonyl Complexes of Zero-Valent Molybdenum. Whereas the differences in steric properties between CNAr^{Mes2} and CNAr^{Dipp2} are illustrated by their coordination behavior toward monovalent Group 11 centers, it was of interest to additionally compare their behavior toward a π-basic metal fragment.[21] Therefore, we next focused on the ability of both CNAr^{Mes2} and CNAr^{Dipp2} to form mixed carbonyl/isocyanide complexes of zero-valent molybdenum. The choice of zero-valent Mo centers as a suitable coordination platform stems from a number of factors. First, there are several examples of isolated Mo(CO)$_n$(CNR)$_m$ ($m = 6 − n$) complexes

(20) We tentatively suggest that the qualitative difference in CNAr^{Dipp2} exchange rates between (κ^2-OTf)Ag(CNAr^{Dipp2})$_2$ and [(THF)$_2$-Cu(CNAr^{Dipp2})$_2$]OTf arises from the larger covalent radius of Ag(I) as compared to that of Cu(I). See the Supporting Information for representative spectra.

(21) For a discussion of the relative π-donor properties of di-, mono-, and zero-valent metal centers towards isocyanides, see: Cotton, F. A.; Zingales, F. *J. Am. Chem. Soc.* **1961**, *83*, 351–355.
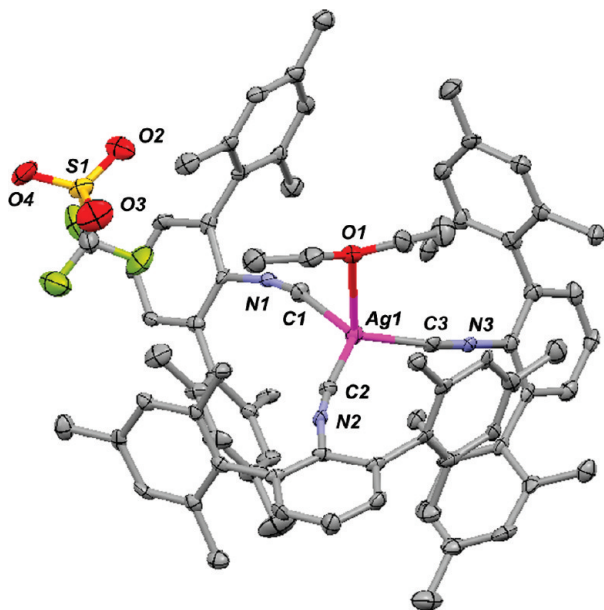
Figure 4. Molecular structure of [(Et$_2$O)Ag(CNAr^{Mes2})$_3$]OTf. Selected bond distances (Å) and angles (deg): C1—Ag1 = 2.188(7); C2—Ag1 = 2.134(8); C3—Ag1 = 2.167(7); O1—Ag1 = 2.673(10); C3—Ag—C1 = 107.0(2); C2—Ag1—C1 = 125.0(3); C2—Ag1—C3 = 122.3(2); O1—Ag1—C1 = 93.2(3); O1—Ag1—C2 = 88.1(2); O1—Ag1—C3 = 114.2(3).

Figure 5. Molecular structure of (κ^2-TfO)Ag(CNAr^{Dipp2})$_2$. Selected bond distances (Å) and angles (deg): Ag1—C1 = 2.083(5); Ag1—C2 = 2.097(6); Ag1—O1 = 2.486(6); Ag1—O2 = 2.568(9); C1—Ag1—C2 = 142.2(2); C1—Ag1—O1 = 107.1(2); C2—Ag1—O1 = 108.4(2); C1—Ag1—O2 = 116.5(2); C2—Ag1—O2 = 95.9(2).

Scheme 4

representing all possible *n* permutations.[4,22–24] Moreover, the strong *trans* directing nature of the CO ligands reliably controls the geometric isomerism of these octahedral complexes. This latter feature of the Mo(CO)$_n$(CNR)$_m$ system is important since deviations from the preferred isocyanide or carbonyl orientations (i.e., *mer* vs *fac* or *cis* vs *trans*) can be readily traced to the steric or electronic influences of bound isocyanide ligands. Further, the presence of the strong CO and CNR oscillators allow the geometrical isomerism in Mo(CO)$_n$(CNR)$_m$ complexes to be conveniently probed by infrared spectroscopy. Because of the geometrical and compositional richness offered by the Mo(CO)$_n$(CNR)$_m$ platform, we were curious to compare not only the differing extent of ligation between CNAr^{Mes2} and CNAr^{Dipp2}, but also the effect of the encumbering *m*-terphenyl group on isocyanide orientation. Indeed, all Mo(CO)$_n$(CNR)$_m$ complexes reported to date have contained isocyanide ligands that are significantly less encumbering than either CNAr^{Mes2} or CNAr^{Dipp2}.

A. Isomeric Modulation of Mo(CO)$_3$(CNR)$_3$ Complexes Utilizing CNAr^{Mes2}. Treatment of *fac*-Mo(CO)$_3$-(NCMe)$_3$ with 3 equiv of CNAr^{Mes2} in toluene leads to

complete consumption of the isocyanide and exclusive formation of the yellow complex *fac*-Mo(CO)$_3$-(CNAr^{Mes2})$_3$ (Scheme 4). The latter was characterized by X-ray diffraction and several views of its molecular structure are displayed in Figure 6. ^{1}H NMR spectra of *fac*-Mo(CO)$_3$(CNAr^{Mes2})$_3$ in C$_6$D$_6$ reveal a single set of Ar^{Mes2} resonances, thereby providing a geometrical consistency between the solid state and solution. In addition, the solution phase (C$_6$D$_6$) FTIR spectrum of *fac*-Mo-(CO)$_3$(CNAr^{Mes2})$_3$ gives rise to two $\nu_{(CO)}$ and two $\nu_{(CN)}$ frequencies as expected for a *fac* conformation.[25] The structure of *fac*-Mo(CO)$_3$(CNAr^{Mes2})$_3$ is remarkable because of the congestion posed by the facial arrangement of the CNAr^{Mes2} ligands. Figure 6 shows *fac*-Mo(CO)$_3$-(CNAr^{Mes2})$_3$ viewed down the trigonal faces defined by both the CO and the CNAr^{Mes2} ligands (a and b,

(22) See for example: (a) Connor, J. A.; Jones, E. M.; McEwen, G. K.; Lloyd, M. K.; McCleverty, J. A. *J. Chem. Soc., Dalton Trans.* **1972**, 1246–1253. (b) Treichel, P. M.; Shaw, D. B. *Inorg. Chim. Acta* **1976**, *16*, 199–202. (c) Albers, M. O.; Coville, N. J.; Ashworth, T. V.; Singleton, E.; Swanpoel, H. E. *J. Organomet. Chem.* **1980**, *199*, 55–62. (d) Hershberger, J. W.; Klingler, R. J.; Kochi, J. K. *J. Am. Chem. Soc.* **1982**, *104*, 3034–3043. (e) Minelli, M.; Maley, W. J. *Inorg. Chem.* **1989**, *28*, 2954–2958. (f) Li, H.; Butler, I. S.; Uhm, H. L. *J. Raman. Spect.* **1992**, *23*, 457–464. (g) Li, H.; Butler, I. S. *Appl. Spectrosc.* **1993**, *47*, 218–221. (h) Lyons, L. J.; Pitz, S. L.; Boyd, D. C. *Inorg. Chem.* **1995**, *34*, 316–322.

(23) (a) Filippou, A. C.; Grünleitner, W. *J. Organomet. Chem.* **1990**, *398*, 99–115. (b) Imhof, W.; Halbauer, K.; Dönnecke, D.; Görls, H. *Acta Crystallogr.* **2006**, *E62*, m462–m464.

(24) For examples *fac*-M(CNR)$_3$(CO)$_3$ containing tridentate, *tris*-isocyanide ligands, see: (a) Hahn, F. E.; Tamm, M. *Angew. Chem., Int. Ed.* **1991**, *30*, 203–205. (b) Hahn, F. E.; Tamm, M. *Organometallics* **1992**, *11*, 84–90. (c) Hahn, F. E.; Tamm, M. *Organometallics* **1994**, *13*, 3002–3008.
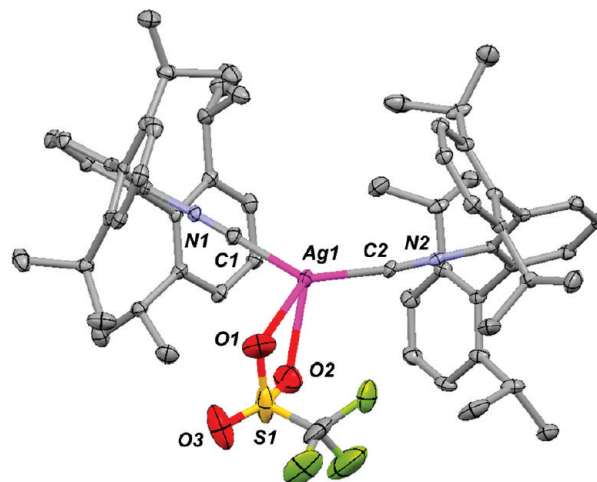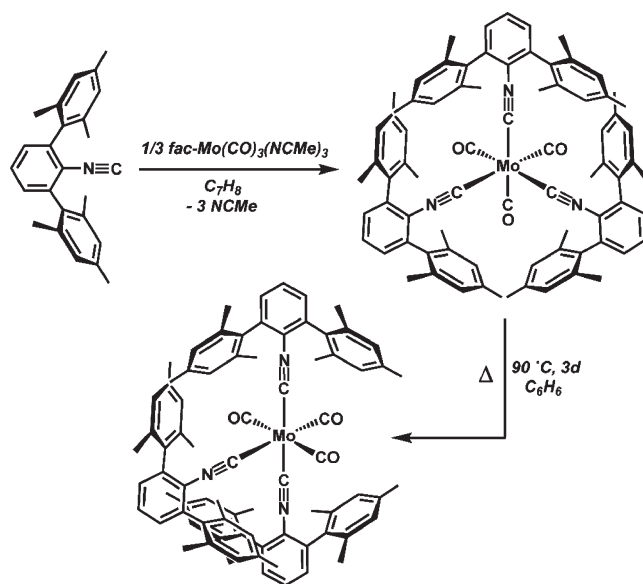
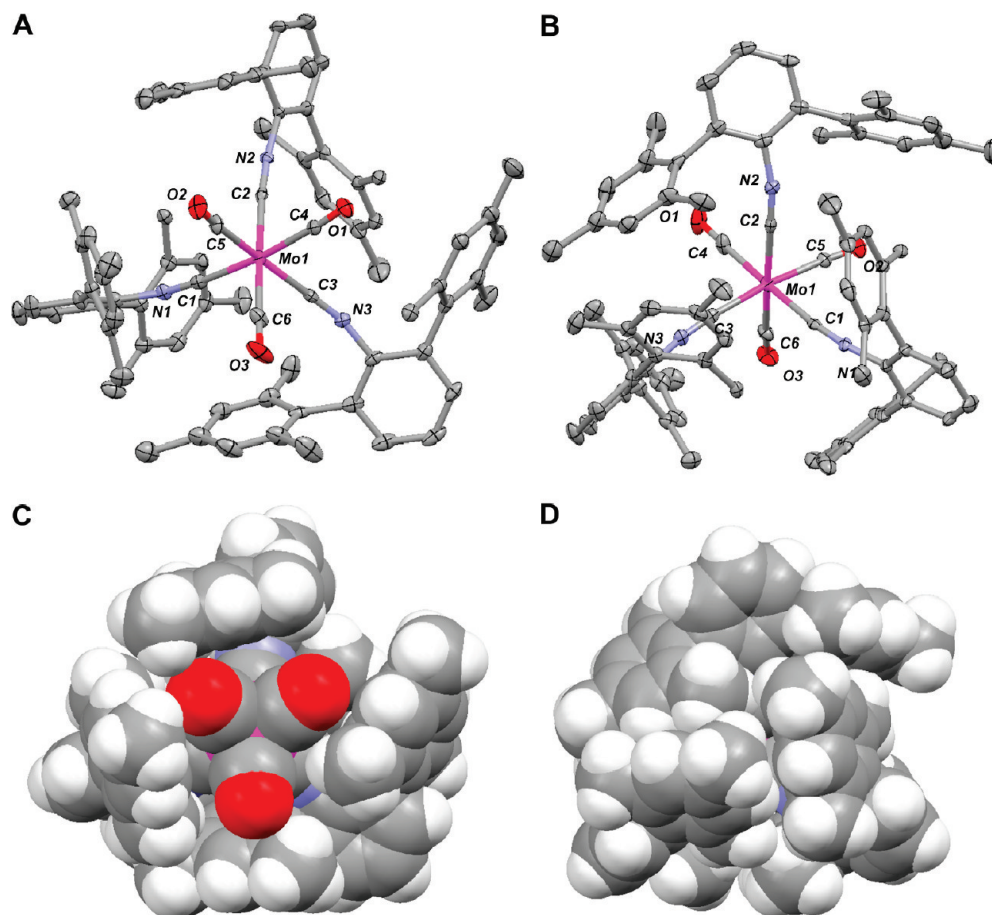(25) King, R. B.; Saran, M. S. *Inorg. Chem.* **1974**, *13*, 74–78.

Figure 6. Molecular structure of *fac*-Mo(CO)$_3$(CNAr^{Mes2})$_3$. (A) View down the trigonal face defined by the three carbonyl ligands. (B) View down the trigonal face defined by the three CNAr^{Mes} ligands. (C) Space filling model corresponding to view A. (D) Space filling model corresponding to view B. Selected bond distances (Å) and angles (deg): Mo1−C1 = 2.106(6); Mo1−C2 = 2.093(6); Mo1−C3 = 2.114(7); Mo1−C4 = 2.015(7); Mo1−C5 = 2.015(7); Mo1−C6 = 2.037(6); C1−Mo1−C2 = 95.1(2); C1−Mo1−C3 = 89.4(2); C1−Mo1−C4 = 178.4(2); C2−Mo1−C3 = 95.6(2); C2−Mo1−C6 = 169.2(2); C3−Mo1−C5 = 173.9(2).

Table 1. Solution $\nu_{(CN)}$ and $\nu_{(CO)}$ Stretching Frequencies for Mixed Isocyanide/Carbonyl Molybdenum Complexes of CNAr^{Mes2} and CNAr^{Dipp2} (C$_6$D$_6$)

complex	$\nu_{(CN)}$ (cm^{-1})	$\nu_{(CO)}$ (cm^{-1})
fac-Mo(CO)$_3$(CNAr^{Mes2})$_3$	2046(s)	1942(s)
	2000(m)	1910(s)
mer-Mo(CO)$_3$(CNAr^{Mes2})$_3$	2046(m)	1926(vs)
	2024(s)	1902(s)
	1993(s)	
trans-Mo(CO)$_4$(CNAr^{Dipp2})$_2$	2054(vs)	1934(vs)
	2007(w)	
trans-Mo(NCMe)(CO)$_3$(CNAr^{Dipp2})$_2$	2021(s)	1932(w)
	1993(s)	1901(s)
		1873(m)
fac,cis-Mo(py)(CO)$_3$(CNAr^{Dipp2})$_2$	2018(s)	1888(s)
	1992(s)	1862(s)
trans-Mo(THF)(CO)$_3$(CNAr^{Dipp2})$_2$	2041(vw)	1924(w)
	2017(m)	1888(s)
	1987(s)	1859(m)

respectively), as well as the corresponding space filling models (c and d). The views down the CNAr^{Mes2} trigonal face clearly show a crowded, interdigitated environment for the Mes substituents. Such congestion suggested that a *fac-mer* isomerization process may be possible to relieve excessive steric pressures. Accordingly, *fac*-Mo(CO)$_3$-(CNAr^{Mes2})$_3$ slowly, but irreversibly, converts to *mer*-Mo(CO)$_3$(CNAr^{Mes2})$_3$ when heated in solution (C$_6$H$_6$, 90 °C, 3 d, Scheme 4). Both ^{1}H NMR and FTIR analysis

of *mer*-Mo(CO)$_3$(CNAr^{Mes2})$_3$ showed the expected spectroscopic signatures for a distinct meridional conformation (Table 1). Crystallographic structure determination (Figure 7) revealed, qualitatively, a significantly less congested coordination environment for *mer*-Mo(CO)$_3$-(CNAr^{Mes2})$_3$ than is found for its *fac* isomer. Notably, extended heating of *mer*-Mo(CO)$_3$(CNAr^{Mes2})$_3$ in C$_6$D$_6$ (100 °C, 2 d) does not lead to degradation or any additional isomerization processes, thus indicating that the *mer* isomer is robust and thermodynamically preferred to the *fac* isomer under the conditions probed.

The preference of Mo(CO)$_3$(CNAr^{Mes2})$_3$ to adopt its meridional isomeric form is particularly noteworthy given that a facial disposition of isocyanide ligands is the preferred coordination geometry in the overwhelming majority of Group 6 M(CO)$_3$(CNR)$_3$ complexes.[22−24] However, as a testament to the small energetic difference that can exist between these geometric isomers, reversible *fac-mer* interconversions have been observed for some M(CO)$_3$(CNR)$_3$ complexes on the ^{1}H NMR time scale.[26] Furthermore, *mer*-M(CO)$_3$(CNR)$_3$ isomers have been isolated in low yield from *fac/mer* mixtures in which the *fac* isomer is the predominant species.[25] We are unaware

(26) Howell, J. A. S.; Yates, P. C.; Ashford, N. F.; Dixon, D. T.; Warren, R. *J. Chem. Soc., Dalton Trans.* **1996**, 3959–3966.
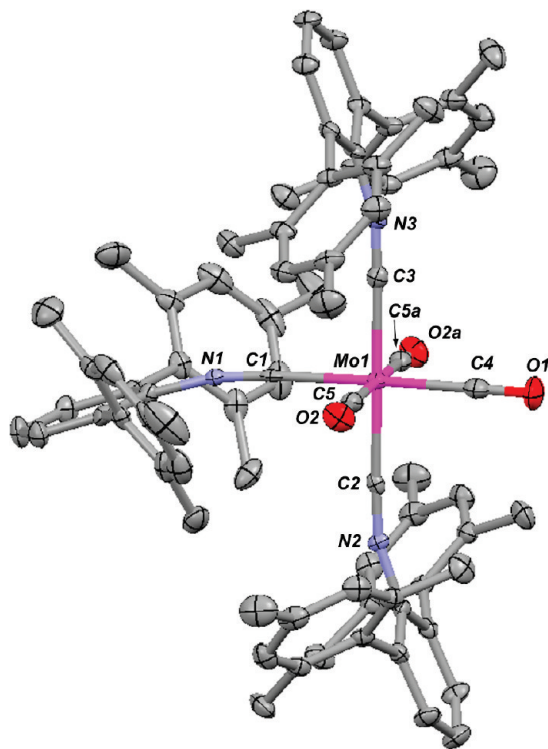
Scheme 5

Figure 7. Molecular structure of *mer*-Mo(CO)$_3$(CNAr^{Mes2})$_3$. Selected bond distances (Å) and angles (deg): Mo1–C1 = 2.118(5); Mo1–C2 = 2.077(5); Mo1–C3 = 2.077(5); Mo1–C4 = 2.025(5); Mo1–C5 = 2.038(4); C1–Mo1–C2 = 89.34(16); C1–Mo1–C3 = 90.41(17); C2–Mo1–C3 = 179.75(17); C1–Mo1–C4 = 178.2(2); C5–Mo1–C5a = 178.4(2).

of an example in which simple thermolysis of a *fac*-M(CO)$_3$(CNR)$_3$ complex provides its *mer*-isomer quantitatively, as is the case for Mo(CO)$_3$(CNAr^{Mes2})$_3$.

In the absence of significant steric pressures, the preference for *fac* over *mer* configurations in Group 6 M(CO)$_3$(CNR)$_3$ complexes may be attributed to an interplay of two electronic factors: (i) the preference for each CNR ligand to be *trans* to the relatively weaker σ-donating CO ligands and (ii) maximization of π-acceptor ability of the CO units in the *fac*-geometry.[27,28] Indeed, the *fac* orientation ensures a triply degenerate configuration wherein each doubly occupied, nonbonding t$_{2g}$-type orbital interacts via π back-bonding with two CO ligands. Such orbital degeneracy is removed in the alternative *mer*-orientation, which renders it the preferred geometry for Jahn–Teller susceptible 17-electron M(CO)$_3$(L)$_3$ complexes.[22h,28,29] However, in only two prior reports has the *mer*-isomer of a neutral, 18-electron Group 6 M(CO)$_3$(CNR)$_3$ complex been reported to form preferentially to its *fac*-isomer.[30,31] In these cases the perfluorinated isocyanides[32] CNCF$_3$ and CNC$_6$F$_5$ were employed. Accordingly, such strongly π-acidic isocyanides may be reasonably expected to withdraw a fair degree of additional electron density from a
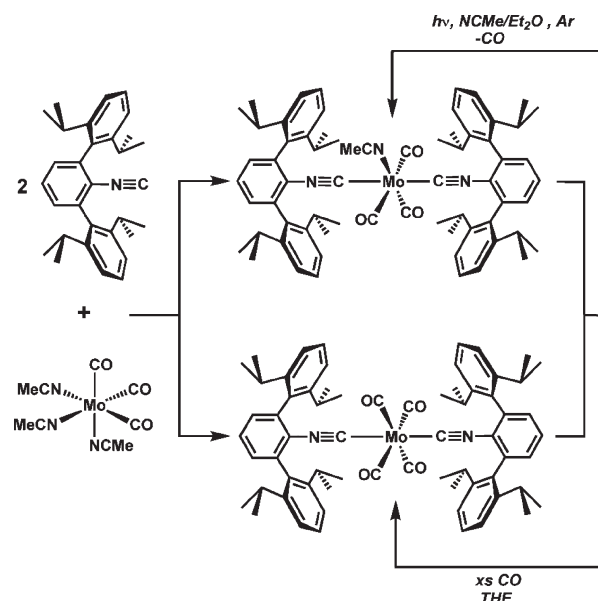
metal center relative to non-fluorinated alkyl or aryl isocyanides. Thus it is interesting to speculate that the strongly π-accepting nature of fluorinated isocyanides enables them to destabilize the *fac*-conformation. In contrast, we suggest that for CNAr^{Mes2}, steric pressures, rather than electronic factors, attendant in placing three encumbering *m*-terphenyl isocyanide units at the face of an octahedron significantly destabilize the *fac*-conformation. Such steric destabilization of octahedral *fac* isomers is known for complexes featuring three phosphine (PR$_3$) ligands of large cone angle.[26]

B. Ligation Control and Isomeric Enforcement by CNAr^{Dipp2} in Mo(CO)$_4$(CNR)$_2$ and Mo(solvento)(CO)$_3$-(CNR)$_2$ Complexes. Unlike CNAr^{Mes2}, treatment of *fac*-Mo(CO)$_3$(NCMe)$_3$ with 3 equiv of the larger CNAr^{Dipp2} leads to a mixture of products and incomplete consumption of the isocyanide. However, when 2 equiv of CNAr^{Dipp2} are employed, a mixture of *trans*-Mo(CO)$_4$-(CNAr^{Dipp2})$_2$ and *trans*-Mo(NCMe)(CO)$_3$(CNAr^{Dipp2})$_2$ is obtained (Scheme 5).[33] Treatment of this mixture with an excess of CO in THF solution generates *trans*-Mo-(CO)$_4$(CNAr^{Dipp2})$_2$ in pure form. Correspondingly, photolysis (Hg lamp, 254 nm) of the mixture under an argon purge in acetonitrile/Et$_2$O (1:1) leads to *trans*-Mo-(NCMe)(CO)$_3$(CNAr^{Dipp2})$_2$ as the exclusive product (Scheme 5). The *trans* configuration of the CNAr^{Dipp2} ligands in both *trans*-Mo(CO)$_4$(CNAr^{Dipp2})$_2$ and *trans*-Mo(NCMe)(CO)$_3$(CNAr^{Dipp2})$_2$ was established by X-ray diffraction (Figures 8 and 9, respectively). In addition, the solution phase (C$_6$D$_6$) FTIR spectrum of *trans*-Mo(CO)$_4$(CNAr^{Dipp2})$_2$ exhibits two ν$_{(CN)}$ stretches and only a single ν$_{(CO)}$ stretch, thereby confirming that the *trans* disposition of the isocyanide ligands can be spectroscopically identified.[34] Notably, however,

(27) Burdett, J. K. *Inorg. Chem.* **1975,** *14,* 375–382.
(28) Mingos, D. M. P. *J. Organomet. Chem.* **1979,** *179,* C29–C33.
(29) For example, see: (a) Bond, A. M.; Colton, R.; Jackowski, J. J. *Inorg. Chem.* **1975,** *14,* 274–278. (b) Bond, A. M.; Colton, R.; Jackowski, J. J. *Inorg. Chem.* **1977,** *16,* 155–159. (c) Bond, A. M.; Colton, R.; Feldberg, S. W.; Mahon, P. J.; Whyte, T. *Organometallics* **1991,** *10,* 3320–3326.
(30) Lentz, D. *J. Organomet. Chem.* **1990,** *381,* 205–212.
(31) Lentz, D.; Anibarro, M.; Preugschat, D.; Bertrand, G. *J. Fluor. Chem.* **1998,** *89,* 73–81.
(32) Lentz, D. *Angew. Chem., Int. Ed.* **1994,** *33,* 1315–1331.

(33) The ratio between *trans*-Mo(CO)$_4$(CNAr^{Dipp2})$_2$ and *trans*-Mo(CO)$_3$-(NCMe)(CNAr^{Dipp2})$_2$ varies with each preparation and has approached equimolar mixtures. We suspect the tetracarbonyl complex Mo(CO)$_4$-(NCMe)$_2$ is present as a contaminant in various extents in the samples of *fac*-Mo(CO)$_3$(NCMe)$_3$ that we prepare.
(34) The alternative *cis*-isomer is expected to exhibit two ν$_{(CN)}$ and four ν$_{(CO)}$ IR active frequencies. See ref 25.
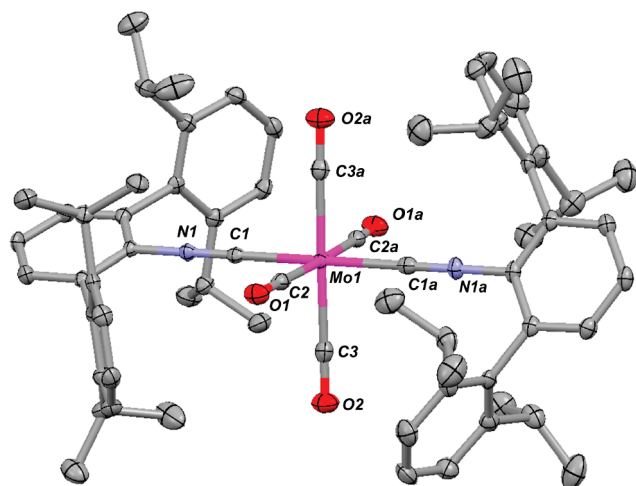
Figure 8. Molecular structure of one crystallographically independent molecule of *trans*-Mo(CO)$_4$(CNAr^{Dipp2})$_2$. Selected bond distances (Å) and angles (deg): Mo1–C1 = 2.087(3); Mo1–C2 2.092(4); Mo1–C3 = 2.043(3); C1–Mo1–C1a = 180.000(2); C1–Mo1–C2 = 91.66(7); C1–Mo1–C3 = 90.61(7); C2–Mo1–C3 = 89.39(7).

Figure 9. One disorder component of the molecular structure of *trans*-Mo(NCMe)(CO)$_3$(CNAr^{Dipp2})$_2$. d(Mo1–C1)=2.083(5) Å. ∠(C1–Mo1–C1a) = 180.000(2)°.

trans-Mo(NCMe)(CO)$_3$(CNAr^{Dipp2})$_2$ crystallized with severe positional disorder between the equatorial CO and NCMe ligands, but the *trans*-disposition of the CNAr^{Dipp2} units is not in question (one component of the disorder model is shown in Figure 9). Furthermore, it is important that *trans*-Mo(NCMe)(CO)$_3$(CNAr^{Dipp2})$_2$ exhibits two $\nu_{(CN)}$ and three $\nu_{(CO)}$ FTIR stretches (C$_6$D$_6$), which is consistent with *trans*-disposed isocyanides and a meridional arrangement of carbonyl ligands.[35]

The *trans*-isocyanide configuration in *trans*-Mo(CO)$_4$-(CNAr^{Dipp2})$_2$ is remarkable given that the *cis*-isomer is observed in the vast majority of Group 6 M(CO)$_4$(CNR)$_2$ complexes.[22,36] We are aware of only two instances of Group 6 M(CO)$_4$(CNR)$_2$ complexes containing *trans*-isocyanides, namely, *trans*-Cr(CNCH$_3$)(CNC$_6$F$_5$)(CO)$_4$ and *trans*-Cr(CNCH$_3$)(CNCF$_3$)(CO)$_4$ both prepared by Lentz et al.[37] Interestingly, whereas the CNC$_6$F$_5$ derivative is obtained in pure form, *trans*-Cr(CNCH$_3$)-(CNCF$_3$)(CO)$_4$ is formed in a 10:1 ratio with its *cis*-isomer. In similar fashion to the tris-isocyanide M(CO)$_3$-(CNR)$_3$ species, the observed tendency of Group 6 M-(CO)$_4$(CNR)$_2$ complexes to adopt a *cis*-isocyanide isomeric form can be rationalized on the basis of placing the isocyanide units *trans* to the weakly σ-donating CO ligands. Furthermore, it has been proposed that fluorination significantly attenuates the σ-donor strength of the isocyanide unit, while concomitantly strengthening its π-acceptor character.[32] Thus, the non-fluorinated CNCH$_3$ ligand may prefer a *trans* orientation with respect to either CNCF$_3$ or CNC$_6$F$_5$. Such arguments, in conjunction with the unique behavior of fluorinated isocyanides mentioned
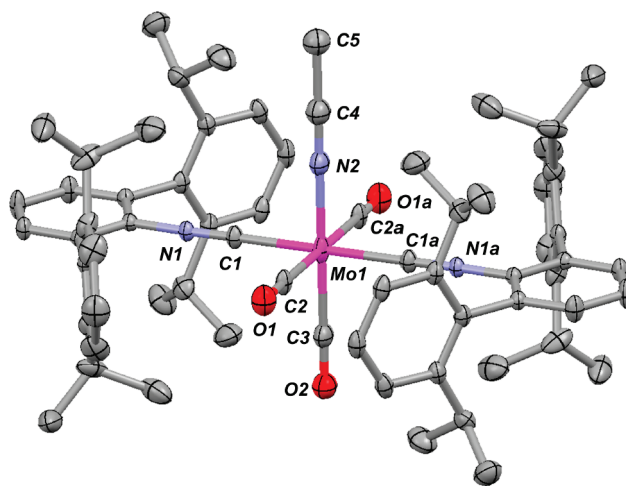
above, may therefore account for the observed *trans*-geometry in *trans*-Cr(CNCH$_3$)(CNC$_6$F$_5$)(CO)$_4$ and *trans*-Cr(CNCH$_3$)(CNCF$_3$)(CO)$_4$. For *trans*-Mo(CO)$_4$-(CNAr^{Dipp2})$_2$, however, we suggest that steric pressures between the Ar^{Dipp2} units are large enough to overcome the electronic penalty of placing the two stronger σ-donating ligands in a *trans* configuration. To this end it is notable that *trans*-Mo(CO)$_4$(CNAr^{Dipp2})$_2$ retains its conformational purity when heated for extended periods, as assayed by solution ^{1}H NMR spectroscopy (C$_6$D$_6$, 90 °C, 24 h).

Tricarbonyl *trans*-Mo(NCMe)(CO)$_3$(CNAr^{Dipp2})$_2$ is noteworthy in that it represents a rare example of a structurally characterized Group 6 nitrile-adduct featuring five strongly π-acidic ligands.[38] Incidentally, *trans*-Mo(NCMe)(CO)$_3$(CNAr^{Dipp2})$_2$ is the first such Mo complex to be structurally characterized. Despite the presence of positional disorder, the solid-state structure of *trans*-Mo(NCMe)(CO)$_3$(CNAr^{Dipp2})$_2$ possesses overall features similar to its tetracarbonyl counterpart, *trans*-Mo-(CO)$_4$(CNAr^{Dipp2})$_2$. Most importantly however, the presence of the labile NCMe ligand in *trans*-Mo(NCMe)-(CO)$_3$(CNAr^{Dipp2})$_2$ allows the opportunity to asses the effect of the encumbering Ar^{Dipp2} units on the substitution chemistry of the [Mo(CO)$_3$(CNR)$_2$] core.[39]

As is the case for the Group 11 complexes described above, three CNAr^{Dipp2} ligands are not accommodated by the [Mo(CO)$_3$] fragment. Thus treatment of *trans*-Mo(NCMe)(CO)$_3$(CNAr^{Dipp2})$_2$ with an additional

(35) For $\nu_{(CO)}$ IR data of several *trans*-M(PR$_3$)$_2$(CO)$_3$L complexes (M = Mo, W), see: Wasserman, H. J.; Kubas, G. J.; Ryan, R. R. *J. Am. Chem. Soc.* **1986**, *108*, 2294–2301.

(36) See for example: (a) Murdoch, H. D.; Henzi, R. *J. Organomet. Chem.* **1966**, *5*, 166–175. (b) Treichel, P. M.; Firsich, D. W.; Essenmacher, G. P. *Inorg. Chem.* **1979**, *18*, 2405–2409. (c) Coville, N. J.; Albers, M. O. *Inorg. Chim. Acta* **1982**, *65*, L7–L8. (d) King, R. B.; Borodinsky, L. *Tetrahedron* **1985**, *41*, 3235–3240. (e) Yang, L.; Cheung, K.-K.; Mayr, A. *J. Organomet. Chem.* **1999**, *585*, 26–34.

(37) Lentz, D.; Pötter, B.; Marschall, R.; Brüdgam, I.; Fuchs, J. *Chem. Ber.* **1990**, *123*, 257–260.

(38) Cambridge Structural Database (CSD v. 5.30, Nov. 2008). (a) Denise, B.; Massoud, A.; Parlier, A.; Rudler, H.; Daran, J. C.; Vaissermann, J.; Alvarez, C.; Patino, R.; Toscano, R. A. *J. Organomet. Chem.* **1990**, *386*, 51–62. (b) Darensbourg, D. J.; Atnip, E. V.; Reidenspies, J. H. *Inorg. Chem.* **1992**, *31*, 4475–4480. (c) Bachman, R. E.; Whitmire, K. H. *Inorg. Chem.* **1995**, *34*, 1542–1551. (d) Jefford, V. J.; Schriver, M. J.; Zaworotko, M. J. *Can. J. Chem.* **1996**, *74*, 107–113. (e) Tang, Y.; Sun, J.; Chen, J. *Organometallics* **1999**, *18*, 2459–2465. (f) Duclos, S.; Conan, F.; Triki, S.; Le Mest, Y.; Gonzalez, M. L.; Sala Pala J. *Polyhedron* **1999**, *18*, 1935–1939. (g) Trylus, K.-H.; Kernbach, U.; Fehlhammer, W. P. *Inorg. Chim. Acta* **1999**, *291*, 266–278.

(39) For comparative reports detailing some substitution chemistry of M(sol)(CO)$_5$ complexes (M = Cr, Mo, W; sol = NCMe, THF), see:(a) Dickson, C.-A.; McFarlane, A. W.; Coville, N. J. *Inorg. Chim. Acta* **1989**, *158*, 205–209. (b) Wieland, S.; van Eldik, R. *Organometallics* **1991**, *10*, 3110–3114.

equivalent of $CNAr^{Dipp2}$ in C_6D_6 solution does not result in the formation of a new species when assayed by ^1H NMR spectroscopy. Rather, ^1H NMR spectra (20 °C) of 1:1 $CNAr^{Dipp2}$/*trans*-Mo(NCMe)(CO)$_3$(CNAr^{Dipp2})$_2$ mixtures reveal static resonances for both species, thereby indicating that rapid isocyanide exchange does not take place on the NMR time scale. In addition, two-dimensional EXSY ^1H NMR experiments did not reveal a slow exchange processes between free and coordinated $CNAr^{Dipp2}$ when mixing times ranging from 50–500 ms were employed.[40] Accordingly, we tentatively suggest that the resistance of *trans*-Mo(NCMe)(CO)$_3$-(CNAr^{Dipp2})$_2$ toward degenerate isocyanide exchange manifests from steric inhibition by the Ar^{Dipp2} substituents of a seemingly associative substitution process.[34] Such a postulate is qualitatively consistent with strong binding of the isocyanide and carbonyl ligands to the π-basic Mo(0) center.

While resistant to substitution by additional $CNAr^{Dipp2}$, *trans*-Mo(NCMe)(CO)$_3$(CNAr^{Dipp2})$_2$ is found to readily react with smaller Lewis bases. Thus treatment of *trans*-Mo(NCMe)(CO)$_3$(CNAr^{Dipp2})$_2$ with an excess of pyridine (py) in C_6H_6 replaces only the coordinated NCMe ligand en route to the complex Mo(py)(CO)$_3$(CNAr^{Dipp2})$_2$ (Scheme 6). Most remarkably, crystallographic analysis revealed that coordination of py induces a *trans→cis* isomerization of the $CNAr^{Dipp2}$ ligands within the [Mo(CO)$_3$(CNAr^{Dipp2})$_2$] core (Figure 10). The *fac,cis* configuration in Mo(py)(CO)$_3$(CNAr^{Dipp2})$_2$ is also indicated from its solution FTIR spectrum, which contains two $\nu_{(CN)}$ and two $\nu_{(CO)}$ stretches. Similar to the Cu(I) and Ag(I) $CNAr^{Dipp2}$ complexes discussed above, steric interferences between the encumbering Ar^{Dipp2} units are clearly evident when the isocyanides are *cis*-disposed. As shown in Figure 10, *fac,cis*-Mo(py)(CO)$_3$(CNAr^{Dipp2})$_2$ features a C_{iso}–Mo–C_{iso} angle of 99.7(3)°, which is fairly obtuse for a nominally octahedral Mo(0) complex featuring six monodentate ligands. Furthermore, that a *cis* orientation can indeed be accommodated by two $CNAr^{Dipp2}$ ligands in an octahedral complex further highlights the preference of *trans*-Mo(CO)$_4$(CNAr^{Dipp2})$_2$ and *trans*-Mo(NCMe)-(CO)$_3$(CNAr^{Dipp2})$_2$ to adopt a *trans*-isocyanide configuration. We suggest that the [Mo(CO)$_3$(CNAr^{Dipp2})$_2$] core converts from a *trans* to *cis* isocyanide configuration to accommodate an increase in electron density at the metal center brought on by the more strongly σ-donating py ligand. Such an interconversion allows both the isocyanide and py groups to be situated *trans* to carbonyl ligands, while also maximizing the π-acceptor ability of the tricarbonyl construct in its facial, rather than meridional, configuration.[27] Lending further credence to this notion is the finding that replacement of the NCMe ligand in *trans*-Mo(NCMe)(CO)$_3$(CNAr^{Dipp2})$_2$ with the weakly σ-donating THF molecule preserves the *trans*-isocyanide configuration as determined by X-ray crystallography[41] and FTIR spectroscopy (Figure 11, Scheme 6). Accordingly, the ability to modulate the geometric isomerism of the [Mo(CNAr^{Dipp2})$_n$] unit by varying ligand donor strength
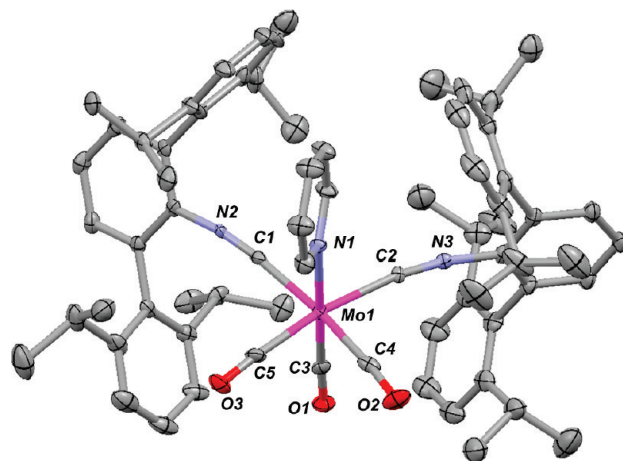
Figure 10. Molecular structure of *cis,fac*-Mo(py)(CO)$_3$(CNAr^{Dipp2})$_2$. Selected bond distances (Å) and angles (deg): Mo1–C1 = 2.160(10); Mo1–C2 = 2.147(8); Mo1–C3 = 1.945(10); Mo1–C4 = 1.949(11); Mo1–C5 = 1.980(11); Mo1–N1 = 2.275(7); C1–Mo1–C2 = 99.7(3); C1–Mo1–N1 = 86.6(3); C2–Mo1–N1 = 90.1(3); C1–Mo1–C5 = 89.7(4); C2–Mo1–C4 = 86.3(4); C4–Mo1–C5 = 84.3(5); C1–Mo1–C4 = 174.0(4); C2–Mo1–C5 = 170.6(4); C3–Mo1–N1 = 179.3(3).

Scheme 6
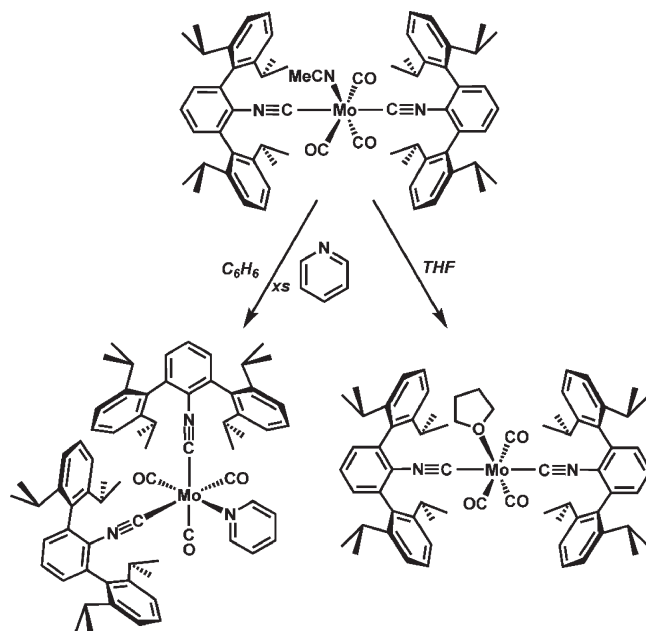
may be potentially beneficial in small molecule activation applications. It is also noteworthy that *trans*-Mo(THF)-(CO)$_3$(CNAr^{Dipp2})$_2$ is only the second structurally characterized Group 6 metal THF-adduct featuring five π-acidic ligands.[42] This fact thus highlights the ability of the $CNAr^{Dipp2}$ unit to stabilize potentially reactive transition metal species.

Concluding Remarks. In conclusion, when compared to the Ar^{Mes2} substituent, the steric properties of the Ar^{Dipp2} group significantly alter the structural and coordination chemistry of complexes supported by *m*-terphenyl

(40) See the Supporting Information.
(41) Similar to the NCMe adduct, *trans*-Mo(THF)(CO)$_3$(CNAr^{Dipp2})$_2$ crystallizes with significant positional disorder between the THF and CO ligands. However, the *trans* disposition of the $CNAr^{Dipp2}$ units is firmly established. One component of the disorder model is depicted in Figure 11.

(42) A search of the Cambridge Structural Database (CSD v. 5.30, Nov. 2008) revealed only one other example, namely, Cr(THF)(CO)$_5$. See: Schubert, U.; Friedrich, P.; Orama, O. *J. Organomet. Chem.* **1978**, *144*, 175–179.

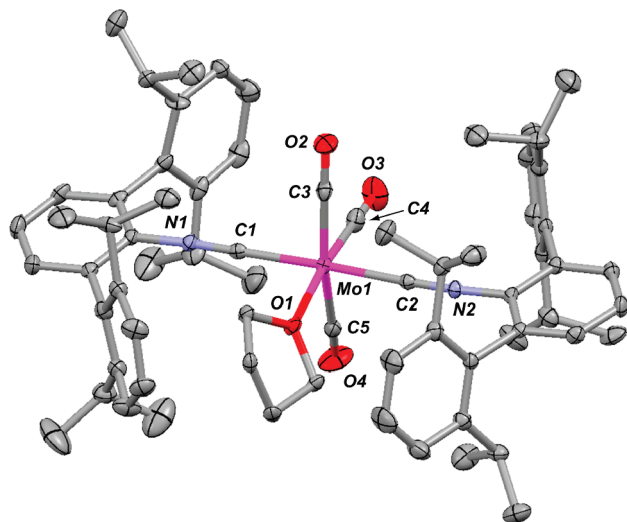**Figure 11.** One disorder component of the molecular structure of *trans*-Mo(THF)(CO)$_3$(CNAr^{Dipp2})$_2$. Selected bond distances (Å) and angles (deg): Mo1−C1 = 2.099(3); Mo1−C2 = 2.087(3); Mo1−C3 = 1.980(4); Mo1−C4 = 1.979(4); Mo1−C2 = 177.03(12); C1−Mo1−C3 = 90.14(13); C1−Mo1−C4 = 93.27(13); C2−Mo1−C3 = 89.69(13); C2−Mo1−C4 = 90.38(13); C3−Mo1−C4 = 84.71(15).

isocyanide ligands. Notably, monovalent Cu and Ag centers and the zero-valent [Mo(CO)$_3$] fragment are seemingly capable of ligating only two CNAr^{Dipp2} units, whereas three less encumbering CNAr^{Mes2} ligands can be readily accommodated. As an added benefit, the steric properties of both CNAr^{Mes2} and CNAr^{Dipp2} can foster unusual coordination environments. This latter feature is exemplified by *mer*-Mo(CO)$_3$(CNAr^{Mes2})$_3$ and *trans*-Mo(CO)$_4$(CNAr^{Dipp2})$_2$, respectively, which represent unique geometrical isomers for mixed isocyanide/carbonyl complexes of zero-valent Mo. Further investigations into the reactivity of the complexes reported here, as well as other transition metal-containing fragments featuring both CNAr^{Mes2} and CNAr^{Dipp2} are ongoing.

Experimental Section

General Considerations. All manipulations were carried out under an atmosphere of dinitrogen using standard Schlenk and glovebox techniques. Solvents were dried and deoxygenated according to standard procedures. Unless otherwise stated, reagent grade starting materials were purchased from commercial sources and used as received. Benzene-d_6 and chloroform-d_1 (Cambridge Isotope Laboratories) were degassed and stored over 4 Å molecular sieves for 2 d prior to use. The isocyanide ligand CNAr^{Mes2},[6] LiAr^{Dipp2},[14] acetic formic anhydride (HC(O)OC(O)Me),[16] TosN$_3$[43] and (C$_6$H$_6$)[Cu(OTf)]$_2$[44] were prepared as described previously. Celite 405 (Fisher Scientific) was dried under vacuum (24 h) at a temperature above 250 °C and stored in the glovebox prior to use. KBr (FTIR grade from Aldrich) was stirred overnight in anhydrous THF, filtered and dried under vacuum (24 h) at a temperature above 250 °C prior to use.

Solution ^{1}H, ^{13}C{^{1}H}, and ^{19}F{^{1}H} NMR spectra were recorded on Varian Mercury 300 and 400 spectrometers or a JEOL ECA-500 spectrometer. ^{1}H and ^{13}C{^{1}H} chemical shifts are reported in ppm relative to SiMe$_4$ (^{1}H and ^{13}C δ = 0.0 ppm) with reference to residual solvent resonances of 7.16 ppm (^{1}H)

and 128.06 ppm (^{13}C) for benzene-d_6 and 7.26 ppm (^{1}H) and 77.1 ppm (^{13}C) for chloroform-d.[45] ^{19}F{^{1}H} NMR spectra were referenced externally to neat trifluoroacetic acid, F$_3$CC(O)OH (δ = −78.5 ppm vs CFCl$_3$ = 0.0 ppm). FTIR spectra were recorded on a Thermo-Nicolet iS10 FT-IR spectrometer. Samples were prepared as either KBr pellets or as C$_6$D$_6$ solutions injected into a ThermoFisher solution cell equipped with NaCl windows. For solution FTIR spectra, solvent peaks were digitally subtracted from all spectra by comparison with an authentic spectrum obtained immediately prior to that of the sample. Combustion analyses were performed by Robertson Microlit Laboratories of Madison, NJ (U.S.A.).

Synthesis of N$_3$Ar^{Dipp2}. To an Et$_2$O solution of LiAr^{Dipp2} (14.72 g, 36.41 mmol, 250 mL) was added an Et$_2$O solution of TosN$_3$ (7.25 g, 36.71 mmol, 1.01 equiv, 75 mL) dropwise via an addition funnel over 2 h. The resulting pale yellow solution was allowed to stir at room temperature for 48 h, after which 100 mL of H$_2$O was added. The organic and aqueous layers were separated, and the latter was washed with Et$_2$O (3 × 200 mL). The combined Et$_2$O extracts were stirred over MgSO$_4$, filtered, and dried in vacuo, affording N$_3$Ar^{Dipp2} as a yellow solid. Yield: 14.94 g, 34.00 mmol, 93%. ^{1}H NMR (400.1 MHz, CDCl$_3$, 20 °C): δ = 7.40 (t, 2H, J = 8 Hz, *p*-Dipp), 7.24 (t, 1H, J = 7 Hz, *p*-Ph), 7.22 (d, 4H, J = 8 Hz, *m*-Dipp), 7.12 (d, 2H, J = 8 Hz, *m*-Ph), 2.67 (sept, 4H, J = 7 Hz, C*H*(CH$_3$)$_2$), 1.15 (d, 12H, J = 7 Hz, CH(C*H$_3$*)$_2$), 1.14 (d, 12H, J = 7 Hz, CH(C*H$_3$*)$_2$) ppm. ^{13}C{^{1}H} NMR (100.6 MHz, CDCl$_3$, 20 °C): δ = 146.7, 130.8, 129.4, 124.6, 123.9, 30.9 (*C*H(CH$_3$)$_2$), 25.0 (CH(*C*H$_3$)$_2$), 23.3 (CH(*C*H$_3$)$_2$) ppm. FTIR (KBr pellet): (ν_{N3}) 2154, 2118, and 2090 cm^{-1} also 3064, 3020, 2959, 2929, 2870, 1580, 1460, 1413, 1382, 1363, 1307, 1279, 1249, 1180, 1052, 935, 841, 805, 794, 760, 685, 669, 608, 585, 553 cm^{-1}. Anal. Calcd For C$_{30}$H$_{37}$N$_3$: C, 81.96; H, 8.48; N, 9.56. Found: C, 81.68; H, 8.43; N, 9.33.

Synthesis of NH$_2$Ar^{Dipp2}. A THF slurry of LiAlH$_4$ (7.61 g, 201 mmol, 5 equiv, 400 mL) was cooled to 0 °C under an N$_2$ atmosphere. To this slurry was added a THF solution of N$_3$Ar^{Dipp2} (17.64 g, 40.20 mmol, 1 equiv, 200 mL) dropwise via cannula over 3 h. Following the addition, the resulting gray/green mixture was refluxed for 12 h. After this period, the reaction mixture was cooled to 0 °C and added dropwise via cannula to 500 mL of an equally cold aqueous 2.0 M solution of KOH. The resulting slurry was filtered through a medium porosity frit to remove insoluble material. The filter cake was then washed with Et$_2$O (3 × 200 mL) and added to the filtrate. The aqueous and organic layers of the filtrate were separated, and the latter was stirred over MgSO$_4$, filtered and dried in vacuo to afford NH$_2$Ar^{Dipp2} as a colorless solid. Yield: 6.78 g, 164 mmol, 82%. ^{1}H NMR (400.1 MHz, CDCl$_3$, 20 °C): δ = 7.37 (t, 2H, J = 8 Hz, *p*-Dipp), 7.25 (d, 4H, J = 8 Hz, *m*-Dipp), 7.97 (d, 2H, J = 8 Hz, *m*-Ph), 6.85 (d, 1H, J = 7 Hz, *p*-Ph), 3.13 (s, 2H, N*H$_2$*), 2.77 (sept, 4H, J = 7 Hz, C*H*(CH$_3$)$_2$), 1.13 (d, 12H, J = 7 Hz, CH(C*H$_3$*)$_2$), 1.11 (d, 12H, J = 7 Hz, CH(C*H$_3$*)$_2$) ppm. ^{13}C{^{1}H} NMR (100.6 MHz, CDCl$_3$, 20 °C): δ = 148.1 (C-NH$_2$), 129.2, 129.4, 125.0, 123.3, 30.6 (*C*H(CH$_3$)$_2$), 24.6 (CH(*C*H$_3$)$_2$), 24.1 (CH(*C*H$_3$)$_2$) ppm. FTIR (KBr pellet): (ν_{NH}) 3472 and 3376 cm^{-1} also 2957, 2926, 2866, 1599, 1460, 1436, 1382, 1367, 1058, 1028, 808, 786, 761, 738 cm^{-1}. Anal. Calcd For C$_{30}$H$_{39}$N: C, 87.10; H, 9.51; N, 3.39. Found: C, 87.39; H, 9.32; N, 3.27.

Synthesis of HC(O)NHAr^{Dipp2}. Neat acetic anhydride (15.86 g, 153 mmol, 8.13 equiv) was cooled to 0 °C under an N$_2$ atmosphere and formic acid (8.79 g, 191.2 mmol, 10 equiv) was added via syringe over 20 min. The resulting colorless solution was refluxed for 3 h at 60 °C and then allowed to cool to room temperature. To this mixture was added a THF solution of NH$_2$Ar^{Dipp2} (7.86 g, 19.1 mmol, 1 equiv) via cannula over 1 h.

(43) McElwee-White, L.; Dougherty, D. A. *J. Am. Chem. Soc.* **1984**, *106*, 3466–3474.

(44) Salomon, R. G.; Kochi, J. K. *J. Am. Chem. Soc.* **1973**, *95*, 3300–3310.

(45) Gottlieb, H. E.; Kotlyar, V.; Nudelman, A. *J. Org. Chem.* **1997**, *62*, 7512–7515.

The reaction mixture was allowed to stir for 36 h after which, 50 mL of H_2O was added. The organic and aqueous layers were then separated, and the latter was washed with Et_2O (3 × 200 mL). The combined Et_2O extracts were stirred over $MgSO_4$, filtered, and dried in vacuo. The resulting residue was then slurried in cold hexanes (100 mL, 0 °C), filtered, and dried in vacuo to afford HC(O)NHAr^{Dipp2} as a colorless solid. Yield: 7.50 g, 16.70 mmol, 87.3%. ^{1}H NMR (400.1 MHz, CDCl$_3$, 20 °C): δ = 7.64 (d, 1H, J = 11 Hz, $HC(O)$), 7.40 (t, 2H, J = 8 Hz, p-Dipp), 7.29 (t, 2H, J = 7 Hz, p-Ph), 7.50 (d, 4H, J = 8 Hz, m-dipp), 7.19 (d, 2H, J = 8 Hz, m-Ph), 6.59 (d, 1H, J = 11 Hz, H-N), 2.62 (sept, 4H, J = 7 Hz, CH(CH$_3$)$_2$) 1.12 (d, 24H, J = 7 Hz, CH(CH_3)$_2$) ppm. ^{13}C{^{1}H} NMR (100.6 MHz, CDCl$_3$, 20 °C): δ = 162.6 (HC(O)N), 146.7, 134.9, 133.4, 131.8, 130.8, 129.4, 124.6, 123.9, 30.9 (CH(CH$_3$)$_2$), 25.0 (CH(CH$_3$)$_2$), 23.3 (CH-(CH$_3$)$_2$) ppm. FTIR (KBr pellet): (ν_{NH}) 3448 cm^{-1}, (ν_{CO}) 1699 cm^{-1} also 3057, 2959, 2882, 2862, 1462, 1424, 1383, 1361, 1324, 1299, 1057, 800, 791, 763, 747 cm^{-1}. Anal. Calcd For C$_{31}$H$_{39}$-NO: C, 84.30; H, 8.91; N, 3.17. Found: C, 83.40; H, 8.88; N, 3.08.

Synthesis of CNAr^{Dipp2}. To a CHCl$_3$ solution of HC-(O)NHAr^{Dipp2} (21.23 g, 48.11 mmol, 1 equiv, 150 mL) was added diisopropylamine (34.31 g, 336.8 mmol, 7 equiv). The solution was cooled to 0 °C under an N$_2$ atmosphere and POCl$_3$ (11 mL, 18.44 g, 120.3 mmol, 2.5 equiv) was added dropwise via syringe. The resulting mixture was allowed to stir for 48 h, after which 150 mL of an aqueous 1.5 M Na$_2$CO$_3$ was transferred via cannula. After an additional 2 h of stirring, the organic and aqueous layers were separated, and the latter was washed with CH$_2$Cl$_2$ (3 × 200 mL). The combined organic extracts were stirred over MgSO$_4$, filtered, and dried in vacuo. The resulting residue was slurried in cold acetonitrile (100 mL, 0 °C), filtered and dried in vacuo to afford isocyanide CNAr^{Dipp2} as a colorless solid. Yield: 18.25 g, 430.7 mmol, 90%. ^{1}H NMR (400.1 MHz, CDCl$_3$, 20 °C): δ = 7.51 (t, 1H, J = 8 Hz, p-Ph), 7.41 (t, 2H, J = 8 Hz, p-Dipp), 7.28 (d, 2H, J = 8 Hz, m-Ph), 6.26 (d, 4H, J = 8 Hz, m-Dipp), 2.54 (sept, 4H, J = 7 Hz, CH(CH$_3$)$_2$), 1.18 (d, 12H, J = 7 Hz, CH(CH_3)$_2$), 1.14 (d, 12H, J = 7 Hz, CH(CH_3)$_2$) ppm. ^{13}C{^{1}H} NMR (100.6 MHz, C$_6$D$_6$, 20 °C): δ = 171.9 (C≡N), 146.7, 139.4, 135.0, 129.7, 129.6, 128.6, 123.4, 31.5 (CH(CH$_3$)$_2$), 24.5 (CH(CH$_3$)$_2$), 24.2 (CH(CH$_3$)$_2$) ppm. FTIR (KBr pellet): (ν_{CN}) 2124 cm^{-1} also 3061, 3025, 2959, 2925, 2867, 1578, 1458, 1417, 1382, 1363, 1328, 1252, 1177, 1055, 1039, 824, 806, 792, 758 cm^{-1}. FTIR (C$_6$D$_6$, NaCl windows): (ν_{CN}) 2118 cm^{-1} also 3062, 3023, 2962, 2929, 2868, 2118, 1616, 1594, 1580, 1460, 1419, 1385, 1363, 1324, 1180, 1052, 811, 794, 760 cm^{-1}. Anal. Calcd For C$_{31}$H$_{37}$N: C, 87.89; H, 8.80; N, 3.31. Found: C, 88.03; H, 8.61; N, 3.12.

Synthesis of [(THF)$_2$Cu(CNAr^{Dipp2})$_2$]OTf. To a THF solution of (C$_6$H$_6$)[CuOTf]$_2$ (0.074 g, 0.147 mmol, 3 mL) was added a THF solution of CNAr^{Dipp2} (0.250 g, 0.590 mmol, 4 equiv, 10 mL). The reaction mixture was allowed to stir for 3 h, after which time all volatile materials were removed under reduced pressure. Dissolution of the resulting colorless residue in THF (5 mL) followed by filtration and storage at −35 °C for 36 h resulted in colorless crystals, which were collected and dried in vacuo. Yield: 0.110 g, 0.091 mmol, 62%. ^{1}H NMR (400.1 MHz, C$_6$D$_6$, 20 °C): δ = 7.34 (t, 4H, J = 8 Hz, p-Dipp), 7.18 (d, 8H, J = 8 Hz, m-Dipp), 6.86 (s, 6H, p-Ph + m-Ph), 3.48 (bs, 8H, THF), 2.51 (setp, 8H, J = 7 Hz, CH(CH$_3$)$_2$), 1.40 (bs, 8H, THF), 1.22 (d, 24H, J = 7 Hz, CH(CH_3)$_2$), 1.06 (d, 24H, J = 7 Hz, CH(CH_3)$_2$) ppm. ^{13}C{^{1}H} NMR (100.6 MHz, C$_6$D$_6$, 20 °C): δ = 166.5 (C≡N), 146.3, 140.3, 133.5, 133.3, 130.2, 130.0, 129.9, 123.7, 31.5 (CH(CH$_3$)$_2$), 24.6 (CH(CH$_3$)$_2$), 24.2 (CH(CH$_3$)$_2$) ppm. ^{19}F{^{1}H} NMR (282.3 MHz, C$_6$D$_6$, 20 °C) δ = −78.3 ppm. FTIR (KBr pellet): (ν_{CN}) 2167 cm^{-1} also 3063, 2964, 2928, 2569, 1578, 1460, 1363, 1315, 1236, 1210, 1027, 757, 636 cm^{-1}. FTIR (C$_6$D$_6$, NaCl windows): (ν_{CN}) 2165 cm^{-1}. Anal. Calcd for C$_{71}$H$_{90}$F$_3$N$_2$O$_5$SCu: C, 70.82; H, 7.53; N, 2.33. Found: C, 71.32; H, 7.34; N, 2.27.

Synthesis of (OTf)Cu(CNAr^{Dipp2})$_2$. To a CH$_2$Cl$_2$ solution of (C$_6$H$_6$)[CuOTf]$_2$ (0.050 g, 0.099 mmol, 3 mL) was added a CH$_2$Cl$_2$ solution of CNAr^{Dipp2} (0.170 g, 0.401 mmol, 4.04 equiv, 5 mL). The reaction mixture was allowed to stir for 3 h, after which all volatile materials were removed under reduced pressure. Dissolution of the resulting colorless residue in CH$_2$Cl$_2$ (3 mL) followed by filtration and storage at −35 °C for 12 h resulted in colorless crystals, which were collected and dried in vacuo. Yield: 0.124 g, 0.117 mmol, 59%. ^{1}H NMR (400.1 MHz, C$_6$D$_6$, 20 °C): δ = 7.34 (t, 4H, J = 8 Hz, p-Dipp), 7.19 (d, 8H, J = 8 Hz, m-Dipp), 6.86 (s, 6H, p-Ph + m-Ph), 2.50 (setp, 8H, J = 6 Hz, CH(CH$_3$)$_2$), 1.21 (d, 24H, J = 6 Hz, CH(CH_3)$_2$), 1.06 (d, 24H, J = 6 Hz, CH(CH_3)$_2$) ppm. ^{13}C{^{1}H} NMR (100.6 MHz, C$_6$D$_6$, 20 °C): δ = 166.5 (C≡N), 146.3, 140.3, 133.5, 133.3, 130.2, 130.0, 129.9, 123.7, 31.5 (CH(CH$_3$)$_2$), 24.6 (CH(CH$_3$)$_2$), 24.2 (CH(CH$_3$)$_2$) ppm. ^{19}F{^{1}H} NMR (282.3 MHz, C$_6$D$_6$, 20 °C): δ = −78.0 ppm. FTIR (KBr pellet): (ν_{CN}) 2167 cm^{-1} also 3063, 2962, 2928, 2869, 1596, 1579, 1460, 1412, 1385, 1364, 1316, 1235, 1209, 1165, 1056, 1020, 806, 757, 636 cm^{-1}. FTIR (C$_6$D$_6$, NaCl windows): (ν_{CN}) 2165 cm^{-1}. (^{13}C{^{1}H} NMR and FTIR signatures for (OTf)Cu(CNAr^{Dipp2})$_2$ and [(THF)$_2$-Cu(CNAr^{Dipp2})$_2$]OTf in C$_6$D$_6$ solution are nearly identical, see above. We attribute this to both THF dissociation in solution and desolvation under prolonged vacuum). Anal. Calcd for C$_{63}$H$_{74}$F$_3$N$_2$O$_3$SCu: C, 71.39; H, 7.04; N, 2.64. Found: C, 71.23; H, 7.12; N, 2.59.

Synthesis of [(Et$_2$O)Ag(CNAr^{Mes2})$_3$]OTf. To a THF solution of AgOTf (0.050 g, 0.196 mmol, 3 mL) was added a THF solution of CNAr^{Mes2} (0.200 g, 0.589 mmol, 3 equiv, 5 mL). The reaction mixture was allowed to stir for 3 h, after which all volatile materials were removed under reduced pressure. Dissolution of the resulting colorless residue in a 15:1 Et$_2$O/THF mixture (4 mL total) followed by filtration and storage at −35 °C for 24 h resulted in colorless crystals, which were collected and dried in vacuo. Yield: 0.162 g, 0.120 mmol, 61%. ^{1}H NMR (400.1 MHz, C$_6$D$_6$, 20 °C): δ = 6.93 (t, 3H, J = 8 Hz, p-Ph), 6.89 (s, 12H, m-Mes), 6.75 (d, 6H, J = 8 Hz, m-Ph), 3.27 (q, 4H, J = 7 Hz, H$_3$CCH_2O), 2.20 (s, 18H, p-CH$_3$), 2.01 (s, 36H, o-CH$_3$), 1.12 (t, 6H, J = 7 Hz, H_3CCH$_2$O) ppm. ^{13}C{^{1}H} NMR (100.6 MHz, C$_6$D$_6$, 20 °C): δ = 140.8, 138.6, 136.0, 134.1, 130.7, 129.9, 129.4, 21.5 (p-CH$_3$-Mes), 20.5 (o-CH$_3$-Mes) ppm (the C≡N resonance was not conclusively identified after prolonged scanning). ^{19}F{^{1}H} NMR (282.3 MHz, C$_6$D$_6$, 20 °C): δ = −77.9 ppm. FTIR (KBr pellet): (ν_{CN}) 2166 cm^{-1}, also 2977, 2947, 2919, 2858, 2613, 1577, 1457, 1379, 1279 cm^{-1}. Anal. Calcd for C$_{80}$H$_{85}$F$_3$N$_3$O$_4$SAg: C, 71.20; H, 6.35; N, 3.11. Found: C, 71.29; H, 6.12; N, 3.19.

Synthesis of (κ^2-OTf)Ag(CNAr^{Dipp2})$_2$. To a THF solution of AgOTf (0.030 g, 0.118 mmol, 5 mL) was added a THF solution of CNAr^{Dipp2} (0.100 g, 0.236 mmol, 5 mL). The reaction mixture was allowed to stir for 3 h, after which all volatile materials were removed under reduced pressure. Dissolution of the resulting colorless residue in an Et$_2$O/n-hexane mixture (1:1, 2 mL total) followed by filtration and storage at −35 °C for 12 h resulted in colorless crystals, which were collected and dried in vacuo. Yield: 0.070 g, 0.063 mmol, 54%. ^{1}H NMR (400.1 MHz, CDCl$_3$, 20 °C): δ = 7.33 (t, 4H, J = 8 Hz, p-Dipp), 7.18 (d, 8H, J = 8 Hz, m-Dipp), 6.9 (t, 1H, J = 9 Hz, m-Ph), 6.8 (t, 1H, J = 9 Hz, m-Ph), 6.80 (d, 4H, J = 7 Hz, p-Ph), 2.43 (sept, 8H, J = 7 Hz, CH(CH$_3$)$_2$), 1.20 (d, 24H, J = 7 Hz, CH(CH_3)$_2$), 1.03 (d, 24H, J = 7 Hz, CH(CH_3)$_2$) ppm. ^{13}C{^{1}H} NMR (100.6 MHz, CDCl$_3$, 20 °C): δ = 169.6 (C≡N), 146.5, 140.4, 133.4, 130.6, 130.3, 130.0, 127.3, 127.1, 123.8, 67.9 (CF$_3$), 31.5 (CH(CH$_3$)$_2$), 24.5 (CH(CH$_3$)$_2$), 24.2 (CH(CH$_3$)$_2$) ppm. ^{19}F{^{1}H} NMR (282.3 MHz, C$_6$D$_6$, 20 °C) δ = −77.7 ppm. FTIR (C$_6$D$_6$, NaCl windows) (ν_{CN}) 2176 cm^{-1} also 3231, 3061, 2962, 2926, 2862, 2390, 2376, 2362, 2174, 1616, 1460, 1333, 1299, 1235, 1221, 1158, 1027, 755, 639 cm^{-1}. Anal. Calcd for C$_{63}$H$_{74}$AgF$_3$N$_2$O$_3$S: C, 68.53; H, 6.76; N, 2.54. Found: C, 70.91; H, 7.26; N, 2.31.

Synthesis of *fac*-Mo(CO)₃(CNAr^Mes2)₃. To a toluene solution of Mo(CO)₃(NCMe)₃ (0.060 g, 0.197 mmol, 4 mL) was added a toluene solution of CNAr^Mes2 (0.200 g, 0.590 mmol, 4 mL). The reaction mixture was allowed to stir for 6 h, after which all volatile materials were removed under reduced pressure. Dissolution of the resulting orange residue in a CH₂Cl₂/*n*-pentane mixture (1:5, 12 mL total) followed by filtration and storage at −35 °C for 24 h resulted in yellow crystals, which were collected and dried in vacuo. Yield: 0.130 g, 0.108 mmol, 50%. ¹H NMR (400.1 MHz, C₆D₆, 20 °C): δ = 6.92 (s, 12H, *m*-Mes), 6.89 (t, 3H, *J* = 7 Hz, *p*-Ph), 6.85 (d, 6H, *J* = 7 Hz, *m*-Ph), 2.25 (s, 18H, *p*-C*H₃*), 2.08 (s, 36H, *o*-C*H₃*) ppm. ¹³C{¹H} NMR (100.6 MHz, C₆D₆, 20 °C): δ = 209.4 (*C*≡O), 175.7 (*C*≡N), 139.0, 137.2, 135.8, 135.0, 130.2, 129.1, 128.4, 127.1, 21.5 (*p*-CH₃-Mes), 20.7 (*o*-CH₃-Mes) ppm. FTIR (C₆D₆, NaCl windows): (ν_CN) 2046 and 2000 cm⁻¹, (ν_CO) 1942 and 1910 cm⁻¹ also 3234, 2920, 2853, 1614, 1579, 1454, 1413, 1375, 1164, 1033, 812, 582 cm⁻¹. Anal. Calcd for C₇₈H₇₅N₃O₃Mo: C, 78.17; H, 6.31; N, 3.51. Found: C, 77.48; H, 6.01; N, 3.48.

Synthesis of *mer*-Mo(CO)₃(CNAr^Mes2)₃. A benzene solution of *fac*-Mo(CO)₃(CNAr^Mes2)₃ (0.100 g, 0.083 mmol, 20 mL) was stirred at 90 °C for 72 h, after which all volatile materials were removed under reduced pressure. Dissolution of the resulting orange residue in a toluene/*n*-pentane mixture (1:3, 4 mL total) followed by filtration and storage at −35 °C for 24 h resulted in orange crystals, which were collected and dried in vacuo. Yield: 0.060 g, 0.050 mmol, 60%. ¹H NMR (400.1 MHz, C₆D₆, 20 °C): δ = 6.98 (s, 4H, *m*-Mes), 6.94 (s, 8H, *m*-Mes), 6.92 (t, 2H, *J* = 8 Hz, *p*-Ph), 6.88 (d, 2H, *J* = 8 Hz, *m*-Ph), 6.87 (t, 1H, *J* = 8 Hz, *p*-Ph), 6.84 (d, 4H, *J* = 8 Hz, *m*-Ph), 2.51 (s, 6H, *p*-CH₃), 2.44 (s, 12H, *p*-CH₃), 2.01 (s, 24H, *o*-CH₃), 2.01 (s, 12H, *o*-CH₃) ppm. ¹³C{¹H} NMR (100.6 MHz, C₆D₆, 20 °C): δ = 211.2 (*C*≡O), 205.1 (*C*≡O), 177.3 (*C*≡N), 175.1 (*C*≡N), 138.8, 138.7, 137.2, 137.1, 135.7, 135.7, 135.2, 134.7, 129.7, 129.5, 129.0, 129.1, 127.2, 126.8, 21.9, and 21.7 (*p*-CH₃-Mes), 20.5 and 20.4 (*o*-CH₃-Mes). FTIR (C₆D₆, NaCl windows): (ν_CN) 2046, 2024, and 1993 cm⁻¹, (ν_CO) 1926 and 1902 cm⁻¹ also 2970, 2948, 2920, 2856, 2359, 2340, 1615, 1576, 1418, 852, 811, 755, 625 cm⁻¹. Anal. Calcd for C₇₈H₇₅N₃O₃Mo: C, 78.17; H, 6.31; N, 3.51. Found: C, 77.50; H, 6.27; N, 4.18.

Formation of Mixtures Containing *trans*-Mo(CO)₄-(CNAr^Dipp2)₂ and *trans*-Mo(NCMe)(CO)₃(CNAr^Dipp2)₂. To an Et₂O solution of *fac*-Mo(CO)₃(NCMe)₃ (0.358 g, 1.180 mmol, 50 mL) was added an Et₂O solution of CNAr^Dipp2 (1.000 g, 2.360 mmol, 2 equiv, 50 mL) and stirred. Over a 24 h period the reaction mixture turned from green to orange resulting in an approximate 1:1 mixture of *trans*-Mo(CO)₄(CNAr^Dipp2)₂ and *trans*-Mo(NCMe)(CO)₃(CNAr^Dipp2)₂ as determined by ¹H NMR analysis.

Synthesis of *trans*-Mo(CO)₄(CNAr^Dipp2)₂. (A). From a mixture of *trans*-Mo(NCMe)(CO)₃CNAr^Dipp2)₂ and *trans*-Mo-(CO)₄CNAr^Dipp2)₂. To a Et₂O solution of *fac*-Mo(CO)₃-(NCMe)₃ (0.072 g, 0.236 mmol, 7 mL) was added an Et₂O solution of CNAr^Dipp2 (0.200 g, 0.472 mmol, 2 equiv, 7 mL). The reaction mixture was allowed to stir for 24 h, after which all volatile materials were removed under reduced pressure. The resulting orange residue was dissolved in 30 mL of THF and CO gas (0.070 mL, 2.909 mmol, 12 equiv) was added. The reaction mixture was stirred for 24 h, after which all the volatile materials were removed under reduced pressure. Dissolution of the resulting yellow residue in a THF/*n*-pentane mixture (3:1, 60 mL total) followed by filtration and storage at −35 °C for 24 h resulted in pale green crystals, which were collected and dried in vacuo. Yield: 0.140 g, 0.133 mmol, 56%.

(B). From isolated *trans*-Mo(NCMe)(CO)₃CNAr^Dipp2)₂. To a THF solution of *trans*-Mo(NCMe)(CO)₃CNAr^Dipp2)₂ (0.100 g, 0.093 mmol, 20 mL) was added CO gas (0.080 mL, 3.326 mmol, 36 equiv) and was then stirred for 24 h. All volatile materials were then removed under reduced pressure. Dissolution of the resulting yellow residue in a THF/*n*-pentane mixture (3:1, 20 mL total) followed by filtration and storage at −35 °C for 24 h resulted in pale green crystals, which were collected and dried in vacuo. Yield: 0.042 g, 0.040 mmol, 42%. ¹H NMR (400.1 MHz, C₆D₆, 20 °C): δ = 7.36 (t, 4H, *J* = 8 Hz, *p*-Dipp), 7.19 (d, 8H, *J* = 8 Hz, *m*-Dipp), 6.91 (d, 4H, *J* = 7 Hz, *m*-Ph), 6.85 (t, 2H, *J* = 6 Hz, *p*-Ph), 2.68 (sept, 8H, *J* = 6 Hz, C*H*(CH₃)₂), 1.33 (d, 24H, *J* = 7 Hz, CH(C*H₃*)₂), 1.06 (d, 24H, *J* = 7 Hz, CH(C*H₃*)₂) ppm. ¹³C{¹H} NMR (100.6 MHz, C₆D₆, 20 °C): δ = 205.4 (*C*≡O), 172.4 (*C*≡N), 146.7, 139.4, 135.1, 129.8, 129.7, 128.8, 127.4, 123.6, 31.6 (*C*H(CH₃)₂), 24.7 (CH(*C*H₃)₂), 24.5 (CH(*C*H₃)₂) ppm. FTIR (C₆D₆, NaCl windows): (ν_CN) 2054, 2007 cm⁻¹, (ν_CO) 1934 cm⁻¹ also 3234, 2961, 2925, 2861, 2387, 2360, 1618, 1454, 1330, 1163, 808 cm⁻¹. Anal. Calcd for C₆₆H₇₄N₂O₄Mo: C, 75.12; H, 7.07; N, 2.66 Found: C, 74.74; H, 7.14; N, 2.63.

Synthesis of *trans*-Mo(NCMe)(CO)₃(CNAr^Dipp2)₂. To an Et₂O solution of *fac*-Mo(CO)₃(NCMe)₃ (0.358 g, 1.180 mmol, 50 mL) was added an Et₂O solution of CNAr^Dipp2 (1.000 g, 2.360 mmol, 2 equiv, 50 mL). The reaction mixture was allowed to stir for 24 h while gradually changing in color from green to orange. Acetonitrile (NCMe, 50 mL) was then added and the reaction mixture was irradiated with a 254 nm Hg lamp under an Ar purge for 24 h. The total volume of the mixture was reduced by half in vacuo resulting in the precipitation of a yellow solid, which was collected by filtration. The yellow precipitate was then slurried in cold acetonitrile (20 mL, 0 °C), filtered, and dried in vacuo to afford *trans*-Mo(NCMe)(CO)₃(CNAr^Dipp2)₂. Yield: 0.703 g, 0.658 mmol, 56%. ¹H NMR (400.1 MHz, C₆D₆, 20 °C): δ = 7.33 (t, 4H, *J* = 7 Hz, *p*-Dipp), 7.19 (d, 8H, *J* = 8 Hz, *m*-Dipp), 6.95 (d, 4H, *J* = 7 Hz, *m*-Ph), 6.87 (t, 2H, *J* = 7 Hz, *p*-Ph), 2.78 (sept, 8H, *J* = 6 Hz, C*H*(CH₃)₂), 1.36 (d, 24H, *J* = 7 Hz, CH(C*H₃*)₂), 1.12 (d, 24H, *J* = 7 Hz, CH(C*H₃*)₂), 1.11 (s, 3H, NCC*H₃*) ppm. ¹³C{¹H} NMR (100.6 MHz, C₆D₆, 20 °C): δ = 216.1 (*C*≡O), 206.7 (*C*≡O), 178.7 (*C*≡N), 146.7, 138.7, 135.6, 129.5, 129.2, 126.1, 123.2, 119.9 (N*C*CH₃), 31.5 (*C*H(CH₃)₂), 24.5 (CH(*C*H₃)₂), 24.4 (CH(*C*H₃)₂), 2.61 (NCC*H₃*) ppm. FTIR (C₆D₆, NaCl windows): (ν_CN) 2021 and 1993 cm⁻¹, (ν_CO) 1932, 1901, and 1873 cm⁻¹ also 2956, 2920, 2861, 2362, 2337, 1579, 1457, 1413, 808, 755 cm⁻¹. Anal. Calcd for C₆₇H₇₇N₃O₃Mo: C, 75.32; H, 7.27; N, 3.93. Found: C, 76.00; H, 7.20; N, 3.80.

Synthesis of *cis*,*fac*-Mo(py)(CO)₃(CNAr^Dipp2)₂. Pyridine (2.000 g, 25.284 mmol, 272 equiv) was added to a benzene solution of Mo(CO)₃(NCMe)₃ (0.100 g, 0.093 mmol, 2 mL). The reaction mixture was allowed to stir for 4 h, after which all volatile materials were removed under reduced pressure. Dissolution of the resulting red residue in an Et₂O/*n*-pentane mixture (1:4, 5 mL total) followed by filtration and storage at −35 °C for 24 h resulted in fine orange crystals, which were collected and dried in vacuo. Yield: 0.071 g, 0.064 mmol, 71%. A very large excess of pyridine is required for the reaction to proceed to completion in a timely fashion. Reaction times of several days are required when employing lesser amounts (e.g., 10 equiv). ¹H NMR (400.1 MHz, C₆D₆, 20 °C): δ = 7.83 (m, 2H, py), 7.34 (t, 4H, *J* = 8 Hz, *p*-Dipp), 7.18 (d, 8H, *J* = 8 Hz, *m*-Dipp), 6.93 (d, 4H, *J* = 7 Hz, *m*-Ph), 6.84 (t, 2H, *J* = 4 Hz, *p*-Ph), 6.81 (m, 1H, p-py), 6.40 (m, 2H, py), 2.71 (sept, 8H, *J* = 7 Hz, C*H*(CH₃)₂), 1.22 (d, 24H, *J* = 7 Hz, CH(C*H₃*)₂), 1.08 (d, 24H, *J* = 7 Hz, CH(C*H₃*)₂) ppm. ¹³C{¹H} NMR (100.6 MHz, C₆D₆, 20 °C): δ = 219.6 (*C*≡O), 207.6 (*C*≡O), 180.2 (*C*≡N), 154.3, 146.4, 138.7, 135.6, 134.2, 129.6, 129.5, 129.2, 126.1, 123.8, 123.4, 31.4 (*C*H(CH₃)₂), 24.6 (CH(*C*H₃)₂), 24.3 (CH(*C*H₃)₂) ppm. FTIR (C₆D₆, NaCl windows): (ν_CN) 2018 and 1992 cm⁻¹, (ν_CO) 1888 and 1862 cm⁻¹ also 3064, 2962, 2928, 2868, 1580, 1459, 1440, 1411, 1380, 1357, 802, 158, 691, 603 cm⁻¹. Anal. Calcd for C₇₀H₇₉N₃O₃-Mo: C, 75.99; H, 7.20; N, 2.34. Found: C, 75.98; H, 7.43; N, 2.79.

Synthesis of *trans*-Mo(THF)(CO)₃(CNAr^Dipp2)₂. A THF solution of *trans*-Mo(NCMe)(CO)₃(CNAr^Dipp2)₂ (0.200 g, 0.182 mmol, 10 mL) was allowed to stir for 12 h and then dried under reduced pressure. This process was then repeated for five

Table 2. Crystallographic Data and Refinement Information

	$CNAr^{Dipp2}$	$[(THF)_2Cu(CNAr^{Dipp2})_2]OTf$	$(OTf)Cu(CNAr^{Dipp2})_2 \cdot 4CH_2Cl_2$
formula	$C_{31}H_{37}N$	$C_{71}H_{90}CuF_3N_2O_5S$	$C_{67}H_{82}Cl_8CuF_3N_2O_3S$
crystal system	monoclinic	monoclinic	monoclinic
space group	$P2_1/n$	$P2_1/c$	$C2/c$
a, Å	12.0083(11)	12.002(5)	22.0775(17)
b, Å	17.2200(16)	34.000(5)	13.8153(12)
c, Å	12.7738(12)	18.363(5)	23.525(2)
α, deg	90	90	90
β, deg	99.3020(10)	107.463(5)	100.020(5)
γ, deg	90	90	90
V, Å^3	2606.7(4)	7148(4)	7065.9(10)
Z	4	4	4
radiation (λ, Å)	Mo Kα, 0.71073	Mo Kα, 0.71073	Cu Kα, 1.54178
ρ (calcd), g/cm^3	1.079	1.119	1.316
μ, mm^{-1}	0.061	0.388	3.917
temp, K	100(2)	100(2)	100(2)
θ max, deg	25.43	23.25	68.13
data/parameters	4812/297	10043/764	6078/425
R_1	0.0404	0.0656	0.0658
wR_2	0.0987	0.1306	0.1729
GOF	1.043	1.030	1.035

	$[(Et_2O)Ag(CNAr^{Mes2})_3]OTf$	$(\kappa^2\text{-}OTf)Ag(CNAr^{Dipp2})_2$	$fac\text{-}Mo(CO)_3(CNAr^{Mes2})_3$
formula	$C_{80}H_{83}AgF_3N_3O_4S$	$C_{63}H_{74}AgF_3N_2O_3S$	$C_{78}H_{75}MoN_3O_3$
crystal system	orthorhombic	orthorhombic	monoclinic
space group	$P2_12_12_1$	$Pbca$	$P2_1/c$
a, Å	14.480(14)	24.7376(14)	23.853(19)
b, Å	19.449(11)	19.1647(11)	12.336(9)
c, Å	25.316(19)	27.0246(16)	24.925(19)
α, deg	90	90	90
β, deg	90	90	103.458(10)
γ, deg	90	90	90
V, Å^3	7129.5	12812.1(13)	7133(9)
Z	4	8	4
radiation (λ, Å)	Mo Kα, 0.71073	Mo Kα, 0.71073	Mo Kα, 0.71073
ρ (calcd.), g/cm^3	1.255	1.145	1.116
μ, mm^{-1}	0.371	0.397	0.230
temp, K	100(2)	100(2)	100(2)
θ max, deg	23.25	23.82	23.53
data/parameters	9918/849	9838/683	10578/784
R_1	0.0583	0.0686	0.0798
wR_2	0.0996	0.1829	0.1645
GOF	1.004	1.062	1.032

	$mer\text{-}Mo(CO)_3(CNAr^{Mes2})_3$	$trans\text{-}Mo(CO)_4(CNAr^{Dipp2})_2$	$trans\text{-}Mo(NCMe)(CO)_3(CNAr^{Dipp2})_2$
formula	$C_{78}H_{75}MoN_3O_3$	$C_{66}H_{74}MoN_2O_4$	$C_{66}H_{77}MoN_3O_3$
crystal system	monoclinic	monoclinic	tetragonal
space group	$P2_1/m$	$C2/c$	$I4/m$
a, Å	12.3865(11)	24.0662(17)	20.7048(5)
b, Å	16.6448(14)	23.9799(17)	20.7048(5)
c, Å	16.2852(14)	21.1907(15)	19.9285(6)
α, deg	90	90	90
β, deg	99.2460(10)	108.3150(10)	90
γ, deg	90	90	90
V, Å^3	3313.9(5)	11609.8(14)	8543.1(4)
Z	2	8	4
radiation (λ, Å)	Mo Kα, 0.71073	Mo Kα, 0.71073	Cu Kα, 1.54178
ρ (calcd.), g/cm^3	1.201	1.207	0.806
μ, mm^{-1}	0.247	0.274	1.491
temp, K	100(2)	100(2)	100(2)
θ max, deg	28.36	27.88	65.97
data/parameters	6054/415	13455/679	3739/232
R_1	0.0516	0.0415	0.0699
wR_2	0.0943	0.0821	0.2205
GOF	1.013	1.009	1.098

	$cis,fac\text{-}Mo(py)(CO)_3(CNAr^{Dipp2})_2 \cdot 1.5Et_2O$	$trans\text{-}Mo(NCMe)(CO)_3(CNAr^{Dipp2})_2 \cdot 2THF$
formula	$C_{76}H_{94}MoN_3O_{4.50}$	$C_{77}H_{98}MoN_2O_6$
crystal system	orthorhombic	monoclinic
space group	$P2_12_12_1$	$P2_1/n$
a, Å	16.6415(11)	16.950(9)

Table 2. Continued

	cis,fac-Mo(py)(CO)$_3$(CNAr^{Dipp2})$_2$·1.5Et$_2$O	*trans*-Mo(NCMe)(CO)$_3$(CNAr^{Dipp2})$_2$·2THF
b, Å	17.4785(12)	17.551(9)
c, Å	24.6126(17)	25.085(13)
α, deg	90	90
β, deg	90	107.81(8)
γ, deg	90	90
V, Å^3	7159.0(8)	7104.9(11)
Z	4	4
radiation (λ, Å)	Mo Kα, 0.71073	Mo Kα, 0.71073
ρ (calcd.), g/cm^3	1.135	1.163
μ, mm^{-1}	0.231	0.235
temp, K	150(2)	100(2)
θ max, deg	27.92	25.57
data/parameters	15976/805	13107 /1101
R_1	0.1094	0.0590
wR_2	0.2237	0.1000
GOF	1.095	1.109

iterations. Dissolution of the resulting orange residue in a toluene/*n*-pentane mixture (1:3, 4 mL total) followed by filtration and storage at −35 °C for 24 h resulted in orange crystals, which were collected and dried in vacuo. Yield: 0.075 g, 0.068 mmol, 53%. ^{1}H NMR (400.1 MHz, C$_6$D$_6$, 20 °C): δ = 7.33 (t, 4H, J = 8 Hz, *p*-Dipp), 7.19 (d, 8H, J = 8 Hz, *m*-Dipp), 6.92 (d, 4H, J = 7 Hz, *m*-Ph), 6.85 (t, 2H, J = 7 Hz, *p*-Ph), 2.78 (sept, 8H, J = 7 Hz, C*H*(CH$_3$)$_2$), 2.66 (bs, 4H, THF), 1.39 (d, 24H, J = 7 Hz, CH(C*H$_3$*)$_2$), 1.29 (bs, 4H, THF), 1.10 (d, 24H, J = 7 Hz, CH(C*H$_3$*)$_2$) ppm. ^{13}C{^{1}H} NMR (100.6 MHz, C$_6$D$_6$, 20 °C): δ = 220.5 (*C*≡O), 207.5 (*C*≡O), 179.6 (*C*≡N), 146.6, 138.7, 135.7, 129.7, 129.2, 126.3, 123.4, 76.5 (THF), 31.4 (*C*H(CH$_3$)$_2$), 26.6 (THF), 24.5 (CH(*C*H$_3$)$_2$), 24.4 (CH(*C*H$_3$)$_2$) ppm. FTIR (C$_6$D$_6$, NaCl windows): (ν_{CN}) 2041, 2018, and 1987 cm^{-1}, (ν_{CO}) 1924, 1888, and 1859 cm^{-1} also 2964, 2925, 2867, 1582, 1463, 1413, 1383, 1363, 752 cm^{-1}. Prolonged exposure to vacuum partially removes the coordinated THF ligand. Accordingly, repeated combustion analyses gave inconsistent results.

Crystallographic Structure Determinations. Single crystal X-ray structure determinations were carried out at low temperature on either a Bruker P4, Platform or Kappa Diffractometer equipped with a Bruker APEX detector. All structures were solved by direct methods with SIR 2004[46] and refined by full-matrix least-squares procedures utilizing SHELXL-97.[47] Crystallographic data collection and refinement information is listed in Table 2. Crystals of *cis,fac*-Mo(py)(CO)$_3$-(CNAr^{Dipp2})$_2$ repeatedly gave rise to poor quality data sets because of the formation of weakly diffracting crystals. The highest quality data set, which is reported here, gave rise to a final R_1 value of 0.1094. However, connectivity is clearly established and a stable anisotropic refinement was achieved for all non-hydrogen atoms. Cambridge Structural Database (CSD) version 5.30 (Nov. 2008) was used for all searches.[48]

Supporting Information Available: Representative ^{1}H NMR and FTIR spectra for exchange reactions, results of database searches, and crystallographic information files (PDF and CIF). This material is available free of charge via the Internet at http://pubs.acs.org.

(46) Burla, M. C.; Caliandro, R.; Camalli, M.; Carrozzini, B.; Cascarano, G. L.; De Caro, L.; Gaicovazzo, C.; Polidori, G.; Spagna, R. *J. Appl. Crystallogr.* **2005**, *38*, 381–388.

(47) Sheldrick, G. M. *Acta Crystallogr.* **2008**, *A64*, 112–122.

(48) Allen, F. H. *Acta Crystallogr.* **2002**, *B58*, 380–388.